

1    **Environmental factors influencing benthic  
2    communities in the oxygen minimum zones  
3    on the Angolan and Namibian margins**

4

5    Ulrike Hanz<sup>1</sup>, Claudia Wienberg<sup>2</sup>, Dierk Hebbeln<sup>2</sup>, Gerard Duineveld<sup>1</sup>, Marc Lavaleye<sup>1</sup>, Katriina  
6    Juva<sup>3</sup>, Wolf-Christian Dullo<sup>3</sup>, André Freiwald<sup>4</sup>, Leonardo Tamborrino<sup>2</sup>, Gert-Jan Reichart<sup>1,5</sup>,  
7    Sascha Flögel<sup>3</sup>, Furu Mienis<sup>1</sup>

8    <sup>1</sup>*NIOZ-Royal Netherlands Institute for Sea Research and Utrecht University, Department of Ocean Systems, Texel,  
9    1797SH, Netherlands*

10    <sup>2</sup>*MARUM–Center for Marine Environmental Sciences, University of Bremen, Bremen, 28359, Germany*

11    <sup>3</sup>*GEOMAR Helmholtz Centre for Ocean Research, Kiel, 24148, Germany*

12    <sup>4</sup>*Department for Marine Research, Senckenberg Institute, Wilhelmshaven, 26382, Germany*

13    <sup>5</sup>*Faculty of Geosciences, Earth Sciences Department, Utrecht University, Utrecht, 3512JE, Netherlands*

14    *Correspondence to: Ulrike Hanz (ulrike.hanz@nioz.nl), +31222369466*

15

16

17

18

19

20

21

22 **Abstract**

23 Thriving benthic communities were observed in the oxygen minimum zones along the southwestern  
24 African margin. On the Namibian margin fossil cold-water coral mounds were overgrown by sponges and  
25 bryozoans, while the Angolan margin was characterized by cold-water coral mounds covered by a living  
26 coral reef. To explain why benthic communities differ in both areas, present day environmental  
27 conditions were assessed, using CTD transects and bottom landers to investigate spatial and temporal  
28 variations of environmental properties. Near-bottom measurements recorded low dissolved oxygen  
29 concentrations on the Namibian margin of 0-0.15 ml l<sup>-1</sup> ( $\triangleq$  0-9 % saturation) and on the Angolan margin  
30 of 0.5-1.5 ml l<sup>-1</sup> ( $\triangleq$  7-18 % saturation), which were associated with relatively high temperatures (11.8-  
31 13.2 °C and 6.4-12.6 °C, respectively). Semi-diurnal barotropic tides were found to interact with the  
32 margin topography producing internal waves. These tidal movements deliver water with more suitable  
33 characteristics to the benthic communities from below and above the zone of low oxygen. Concurrently,  
34 the delivery of high quantity and quality organic matter was observed, being an important food source  
35 for the benthic fauna. On the Namibian margin organic matter originated directly from the surface  
36 productive zone, whereas on the Angolan margin the geochemical signature of organic matter  
37 suggested an additional mechanism of food supply. A nepheloid layer observed above the cold-water  
38 corals may constitute a reservoir of organic matter, facilitating a constant supply of food particles by  
39 tidal mixing. Our data suggest that the benthic fauna on the Namibian margin as well as the cold-water  
40 coral communities on the Angolan margin may compensate for unfavorable conditions of low oxygen  
41 levels and high temperatures with enhanced availability of food, while anoxic conditions on the  
42 Namibian margin are at present a limiting factor for cold-water coral growth. This study provides an  
43 example of how benthic ecosystems cope with such extreme environmental conditions since it is  
44 expected that oxygen minimum zones will expand in the future due to anthropogenic activities.

45

46

47 **1. Introduction**

48 Cold-water corals (CWCs) form 3D structures in the deep-sea, providing important habitats for dense  
49 aggregations of sessile and mobile organisms ranging from mega- to macrofauna (Henry and Roberts,  
50 2007; van Soest et al., 2007) and fish (Costello et al., 2005). Consequently, CWC areas are considered as  
51 deep-sea hotspots of biomass and biodiversity (Buhl-Mortensen et al., 2010; Henry and Roberts, 2017).  
52 Moreover, they form hotspots for carbon cycling by transferring carbon from the water column towards  
53 associated benthic organisms (Oevelen et al., 2009; White et al., 2012). Some framework-forming  
54 scleractinian species, with *Lophelia pertusa* and *Madrepora oculata* being the most common species in  
55 the Atlantic Ocean (Freiwald et al., 2004; White et al., 2005; Roberts et al., 2006; Cairns, 2007), are  
56 capable of forming large elevated seabed structures, so called coral mounds (Wilson, 1979; Wienberg  
57 and Titschack, 2017; Titschack et al., 2015; De Haas et al., 2009). These coral mounds, consisting of coral  
58 debris and hemipelagic sediments, commonly reach heights between 20 and 100 m and can be several  
59 kilometers in diameter. They are widely distributed along the North Atlantic margins, being mainly  
60 restricted to water depths between 200-1000 m, while records of single colonies of *L. pertusa* are  
61 reported from a broader depth range of 50-4000 m depth (Roberts et al., 2006; Hebbeln et al., 2014;  
62 Davies et al., 2008; Mortensen et al., 2001; Freiwald et al., 2004; Freiwald, 2002; Grasmueck et al., 2006;  
63 Wheeler et al., 2007).

64 A global ecological-niche factor analysis by Davies et al. (2008) and Davies and Guinotte (2011),  
65 predicting suitable habitats for *L. pertusa*, showed that this species generally thrives in areas which are  
66 nutrient-rich, well oxygenated and affected by relatively strong bottom water currents. Other factors  
67 potentially important for proliferation of *L. pertusa* include chemical and physical properties of the  
68 ambient water masses, like for example aragonite saturation state, salinity and temperature (Davies et  
69 al., 2008; Dullo et al., 2008; Flögel et al., 2014; Davies and Guinotte, 2011). *L. pertusa* is most commonly  
70 found at temperatures between 4-12 °C and a very wide salinity range between 32 and 38.8 (Freiwald et  
71 al., 2004). The link of *L. pertusa* to particular salinity and temperature within the NE Atlantic led Dullo et  
72 al. (2008) to suggest that they are restricted to a specific density envelope of sigma-theta ( $\sigma\Theta$ ) = 27.35-  
73 27.65 kg m<sup>-3</sup>. In addition, the majority of occurrences of live *L. pertusa* comes from sites with dissolved  
74 oxygen concentrations (DO<sub>conc</sub>) between 6-6.5 ml l<sup>-1</sup> (Davies et al., 2008), with lowest recorded oxygen  
75 values being 2.1-3.2 ml l<sup>-1</sup> at CWC sites in the Gulf of Mexico (Davies et al., 2010; Schroeder, 2002;  
76 Brooke and Ross, 2014) or even as low as 1-1.5 ml l<sup>-1</sup> off Mauritania where CWC mounds are in a  
77 dormant stage showing only scarce living coral occurrences today (Wienberg et al., 2018; Ramos et al.,  
78 2017). Dissolved oxygen levels hence seem to affect the formation of CWC structures as was also shown

79 by Holocene records obtained from the Mediterranean Sea, which revealed periods of reef demise and  
80 growth in conjunction with hypoxia (with  $2 \text{ ml l}^{-1}$  seemingly forming a threshold value for active coral  
81 growth (Fink et al., 2012).

82 Another essential constraint for CWC growth and therefore mound development in the deep-sea is food  
83 supply. *L. pertusa* is an opportunistic feeder, exploiting a wide variety of different food sources,  
84 including phytodetritus, phytoplankton, mesozooplankton, bacteria and dissolved organic matter  
85 (Kiriakoulakis et al., 2005; Dodds et al., 2009; Gori et al., 2014; Mueller et al., 2014; Duineveld et al.,  
86 2007). Not only quantity but also quality of food particles is of crucial importance for the uptake  
87 efficiency as well as ecosystem functioning of CWCs (Ruhl, 2008; Mueller et al., 2014). Transport of  
88 surface organic matter towards CWC sites at intermediate water depths has been found to involve  
89 either active swimming (zooplankton), passive sinking, advection, local downwelling, and internal waves  
90 and associated mixing processes resulting from interactions with topography (Davies et al., 2009; van  
91 Haren et al., 2014; Thiem et al., 2006; White et al., 2005; Mienis et al., 2009; Frederiksen et al., 1992).  
92 With worldwide efforts to map CWC communities, *L. pertusa* was also found under conditions which are  
93 environmentally stressful or extreme in the sense of the global limits defined by Davies et al. (2008) and  
94 Davies and Guinotte (2011). Examples are the warm and salty waters of the Mediterranean and the high  
95 bottom water temperatures along the US coast (Cape Lookout; (Freiwald et al., 2009; Mienis et al.,  
96 2014; Taviani et al., 2005). Environmental stress generally increases energy needs for organisms to  
97 recover and maintain optimal functioning, which accordingly increases their food demand (Sokolova et  
98 al., 2012).

99 For the SW African margin one of the few records of living CWC comes from the Angolan margin (at  $7^\circ \text{ S}$ ;  
100 (Le Guilloux et al., 2009), which raises the question whether environmental factors limit CWC growth  
101 due to the presence of an Oxygen Minimum Zone (OMZ; see Karstensen et al. 2008), or whether this is  
102 related to a lack of data. Hydroacoustic campaigns revealed extended areas off Angola and Namibia with  
103 structures that morphologically resemble coral mound structures known from the NE Atlantic (M76-3,  
104 MSM20-1; Geissler et al., 2013; Zabel et al., 2012). Therefore two of such mound areas on the margins  
105 off Namibia and Angola were visited during the RV *Meteor* cruise M122 'ANNA' (ANgola/NAmibia) in  
106 January 2016 (Hebbeln et al., 2017). During this cruise fossil CWC mound structures were found near  
107 Namibia, while flourishing CWC reef covered mound structures were observed on the Angolan margin.  
108 The aim of the present study was to assess present-day environmental conditions at the southwestern  
109 African margin to identify why CWCs thrive on the Angolan margin and are absent on the Namibian

110 margin. Key parameters influencing CWCs, hydrographic parameters as well as chemical properties of  
111 the water column were measured to characterize the difference in environmental conditions and food  
112 supply. These data are used to provide new insights in susceptibility of CWCs towards extreme oxygen  
113 limited environments, in order to improve understanding of the fate of CWC mounds in a changing  
114 ocean.

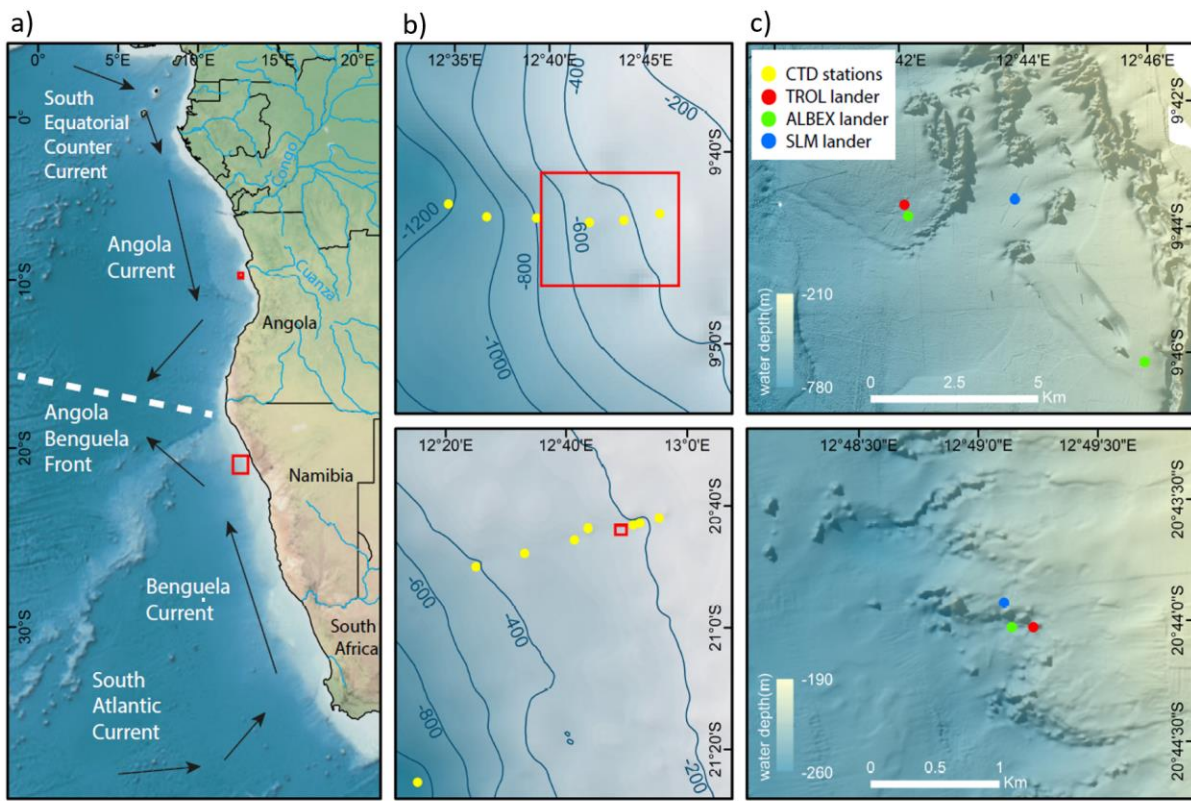
## 115 2. Material and Methods

### 116 2.1 Setting

#### 117 2.1.1 Oceanographic setting

118 The SW African margin is one of the four major eastern boundary regions in the world and is  
119 characterized by upwelling of nutrient-rich cold waters (Shannon and Nelson, 1996). The availability of  
120 nutrients triggers a high primary production, making it one of the most productive marine areas  
121 worldwide with an estimated production of 0.37 Gt C/yr (Carr and Kearns, 2003). Remineralization of  
122 high fluxes of organic particles settling through the water column results in severe mid-depth oxygen  
123 depletion and an intense OMZ over large areas along the SW African margin (Chapman and Shannon,  
124 1985). The extension of the OMZs is highly dynamic being controlled by upwelling intensity, which  
125 depends on the prevailing winds and two current systems along the SW African margin, i.e. the Benguela  
126 and the Angola currents (Kostianoy and Lutjeharms, 1999; Chapman and Shannon, 1987; Fig. 1). The  
127 Benguela Current originates from the South Atlantic Current, which mixes with water from the Indian  
128 Ocean at the southern tip of Africa (Poole and Tomczak, 1999; Mohrholz et al., 2008; Rae, 2005) and  
129 introduces relatively cold and oxygen-rich Eastern South Atlantic Central Water (ESACW; Poole and  
130 Tomczak 1999) to the SW African margin (Mohrholz et al., 2014). The Angola Current originates from the  
131 South Equatorial Counter Current and introduces warmer, nutrient-poor and less oxygenated South  
132 Atlantic Central Water (SACW; Poole and Tomczak (1999) to the continental margin (Fig. 1a). SACW is  
133 defined by a linear relationship between temperature and salinity in a T-S plot (Shannon et al., 1987).  
134 While the SACW flows along the continental margin the oxygen concentration is decreasing  
135 continuously due to remineralisation processes of organic matter on the SW African shelf (Mohrholz et  
136 al., 2008). Both currents converge at around 14-16 °S, resulting in the Angola-Benguela Front  
137 (Lutjeharms and Stockton, 1987). In austral summer, the Angola-Benguela Front can move southward to  
138 23 °S (Shannon et al., 1986), thus increasing the influence of the SACW along the Namibian coast (Junker  
139 et al., 2017; Chapman and Shannon, 1987), contributing to the pronounced OMZ due to its low initial  
140 oxygen concentration (Poole and Tomczak, 1999). ESACW is the dominant water mass at the Namibian

141 margin during the main upwelling season in austral winter, expanding from the oceanic zone about 350  
 142 km offshore, further in-shore. (Mohrholz et al., 2014). The surface water mass at the Namibian margin is  
 143 a mixture of sun warmed upwelled water and water of the Agulhas Current, which mixes in complex  
 144 eddies and filaments and is called South Atlantic Subtropical Surface Water (SASSW) (Hutchings et al.,  
 145 2009). At the Angolan margin the surface water is additionally influenced by water from the Cuanza and  
 146 Congo rivers (Kopte et al., 2017, Fig. 1). Antarctic Intermediate Water (AAIW) is situated in deeper areas  
 147 at the African continental margin and can be identified as the freshest water mass around 700-800 m  
 148 depth (Shannon and Nelson, 1996).



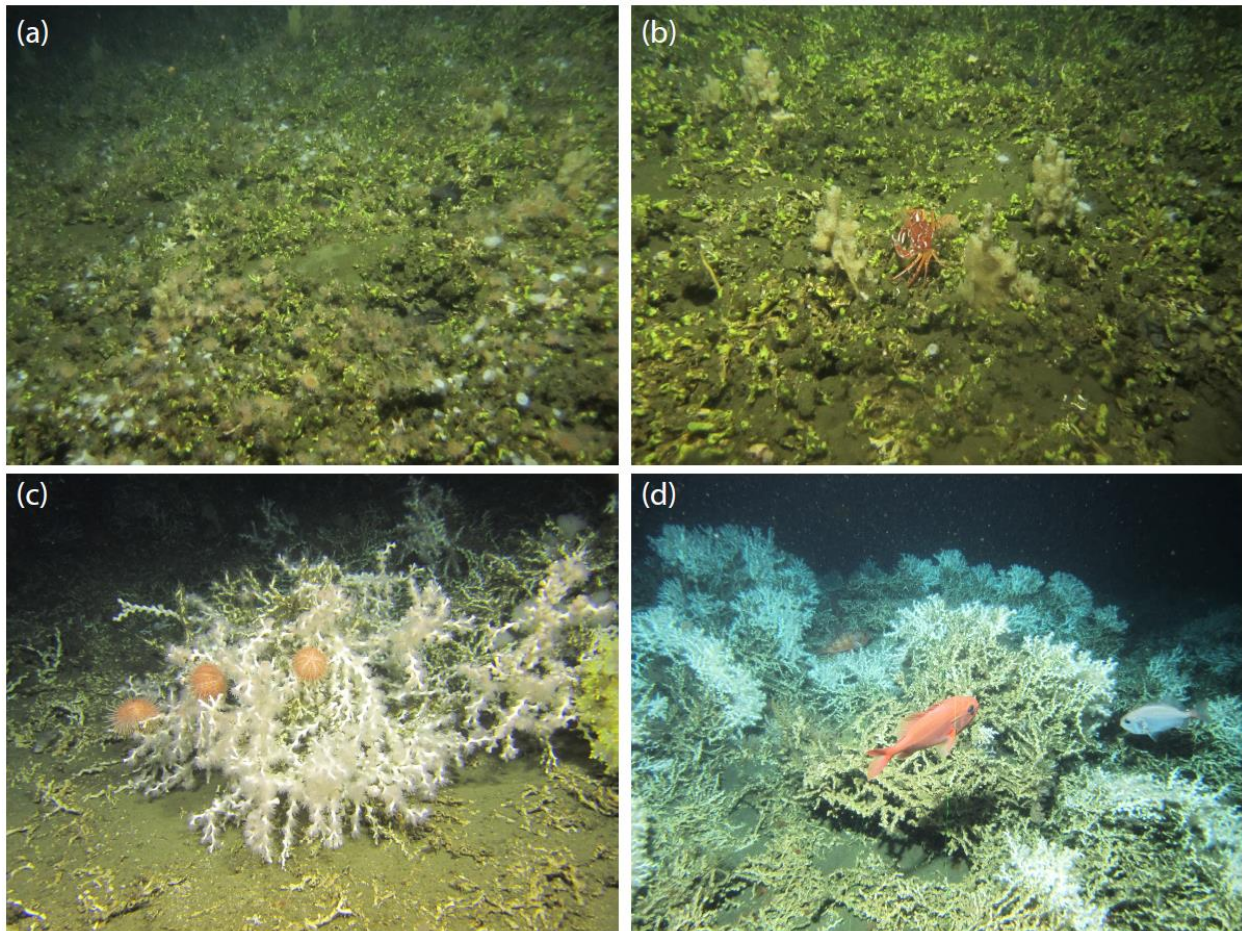
149  
 150 **Figure 1** (a) Overview map showing the research areas off Angola and Namibia (red squares) and main features of the surface  
 151 water circulation (arrows) and frontal zone (dashed line) as well as the two main rivers discharging at the Angolan margin.  
 152 Detailed bathymetry maps of the Angolan (upper maps) and Namibian margins (lower maps) showing the position of (b) CTD  
 153 transects (note the deep CTD cast down to 1000 m water depth conducted off Namibia) and (c) bottom lander deployments  
 154 (red squares shown in (b) indicate the cutouts displayed in (c)).

### 155 2.1.2. Coral mounds along the Angolan and Namibian margins

156 During RV *Meteor* cruise M122 in 2016, over 2000 coral mounds were observed between 160-260 m  
 157 water depth on the Namibian shelf (Hebbeln et al., 2017). All mounds were densely covered with coral

158 rubble and dead coral framework, while no living corals were observed in the study area (Hebbeln et al.,  
159 2017; Figs. 2a, b). Few species were locally very abundant, viz. a yellow cheilostome bryozoan which was  
160 the most common species, and five sponge species. The bryozoans were encrusting the coral rubble,  
161 whereas some sponge species reached heights of up to 30 cm (Fig. 2a, b). The remaining community  
162 consisted of an impoverished fauna overgrowing *L. pertusa* debris. Commonly found sessile organism  
163 were actiniarians, zoanthids, hydroids, some thin encrusting sponges, serpulids and sabellid polychaetes.  
164 The mobile fauna comprised asteroids, ophiuroids, two shrimp species, amphipods, cumaceans and  
165 holothurians. Locally high abundances of *Suffogobius bibarbatus*, a fish that is known to be adapted to  
166 hypoxic conditions, were observed in cavities underneath the coral framework (Hebbeln, 2017). Dead  
167 corals collected from the surface of various Namibian mounds date back to about 5 ka BP, pointing to a  
168 simultaneous demise of these mounds during the mid-Holocene (Tamborrino et al., accepted).

169 On the Angolan margin CWC structures varied from individual mounds to long ridges. Some mounds  
170 reached heights of more than 100 m above the seafloor. At shallow depths (~250 m) also some isolated  
171 smaller mounds were present (Hebbeln et al. 2017). All mounds showed a thriving CWC cover, which  
172 was dominated by *L. pertusa* (estimated 99% relative abundance), *M. oculata* and solitary corals.  
173 Mounds with a flourishing coral cover were mainly situated at water depths between 330-470 m,  
174 whereas single colonies were found over an even broader depth range between 250-500 m (Figs. 2c, d;  
175 Hebbeln et al., 2017). Additionally, large aggregations of hexactinellid sponges (*Aphrocallistes*,  
176 *Sympagella*) were observed. First estimates for coral ages obtained from a gravity core collected at one  
177 of the Angolan coral mounds revealed continuous coral mound formation during the last 34 ka until  
178 today (Wefing et al., 2017).



179

180 **Figure 2** ROV images (copyright MARUM ROV SQUID, Bremen, Germany) showing the surface coverage of cold-water coral  
 181 mounds discovered off Namibia (a, b) and Angola (c, d). Images were recorded and briefly described for their faunal  
 182 composition during RV *Meteor* cruise M122 "ANNA" (see Hebbeln et al. 2017). (a) Sylvester mound, 225 m water depth. Dead  
 183 coral framework entirely consisting of *L. pertusa*. The framework is intensely colonized by the yellow bryozoan *Metropriella* sp.,  
 184 zoanthids, actinarians and sponges. Vagile fauna consists of asteroids and gobiid fishes (*Sufflogobius bibarbatus*) that hide  
 185 between hollows underneath the coral framework. (b) Sylvester mound, 238 m water depth. Dense coral rubble (*L. pertusa*)  
 186 heavily overgrown by *Metropriella* sp. and sponges. Note the decapod crab *Macropipus australis* (center of the image). (c)  
 187 Valentine mound, 238 m water depth. Live *L. pertusa* colony being grazed by echinoids. Note the sponge *Aphrocallistes* sp. with  
 188 its actinarian symbionts (right side of the image). (d) Buffalo mound, 345 m water depth. Living CWC reef observed on top of an  
 189 Angolan coral mound. Many fishes are present around the reef (*Helicolenus dactylopterus*, *Gephyroberyx darwini*).

190 **2.2 Methodology**

191 During RV *Meteor* expedition M122 in January 2016, two CTD transects and three short-term bottom  
 192 lander deployments (Table 1, Fig. 1) were carried out to measure environmental conditions influencing  
 193 benthic habitats. In addition, weather data were continuously recorded by the RV *Meteor* weather  
 194 station, providing real-time information on local wind speed and wind direction.

195 2.2.1 *Lander deployments*  
196 Sites for deployment of the NIOZ designed lander (ALBEX) were selected based on multibeam  
197 bathymetric data. On the Namibian margin the bottom lander was deployed on top of a mound  
198 structure (water depth 220 m). Off Angola the lander was deployed in the relatively shallow part of the  
199 mound zone at 340 m water depth and in the deeper part at 530 m (Fig. 1, Table 1). A second lander  
200 (TROL) was deployed simultaneously to the ALBEX lander during two deployments, whereas recorded  
201 data was very similar to the ALBEX data and is not shown here. Additionally, a GEOMAR Satellite Lander  
202 Module (SLM) was deployed off-mound in 230 m depth at the Namibian margin and at 430 m depth at  
203 the Angolan margin (Fig. 1, Table 1). The lander was equipped with an ARO-USB oxygen sensor (JFE-  
204 Advantech™), a combined OBS-fluorometer (Wetlabs™) and an Aquadopp (Nortek™) profiling current  
205 meter. The lander was furthermore equipped with a Technicap PPS4/3 sediment trap with 12 bottles  
206 (allowing daily samples) and a McLane particle pump (24 filter units for each 7.5 L of seawater, two hour  
207 interval) to sample particulate organic matter in the near-bottom water (40 cm above bottom).

208 The SLM was equipped with a 600 kHz ADCP Workhorse Sentinel 600 from RDI, a CTD (SBE SBE16V2™), a  
209 combined fluorescence and turbidity sensor (WET Labs ECO-AFL/FL), a dissolved oxygen sensor (SBE™)  
210 and a pH sensor (SBE™) (Hebbeln et al., 2017). From the SLM only pH measurements are used here,  
211 complementing the data from the NIOZ lander.

212 2.2.2 *CTD transects*  
213 Vertical profiles of hydrographic parameters in the water column, viz. temperature, conductivity, oxygen  
214 and turbidity, were obtained using a Seabird CTD/Rosette system (Seabird SBE 9 plus). The additional  
215 sensors on the CTD were a dissolved oxygen sensor (SBE 43 membrane-type DO Sensor) and a combined  
216 fluorescence and turbidity sensor (WET Labs ECO-AFL/FL). The CTD was combined with a rosette water  
217 sampler consisting of 24 Niskin® water sampling bottles (10 L). CTD casts were carried out along two  
218 downslope CTD transects (Fig. 1). Turbidity data were due to technical problems only collected on the  
219 Angolan slope.

220 2.2.3 *Hydrographic data processing*  
221 The CTD data were processed using the processing software Seabird data SBE 11plus V 5.2 and were  
222 visualized using the program Ocean Data View (Schlitzer (2011); Version 4.7.8).

223 Hydrographic data recorded by the landers were analyzed and plotted using the program R (R Core  
224 Team, 2017). Data from the different instruments (temperature, turbidity, current speed, oxygen

225 concentration, fluorescence) were averaged over a period of 1.5 h to remove shorter term trends and  
226 occasional spikes. Correlations between variables were assessed by Spearman's rank correlation tests.

227 *2.2.4 Suspended particulate matter*

228 Near-bottom suspended particulate organic matter (SPOM) was sampled by means of a phytoplankton  
229 sampler (McLane PPS) mounted on the ALBEX lander. The PPS was fitted with 24 GF/F filters (47 mm  
230 Whatman™ GF/F filters pre-combusted at 450 °C). A maximum of 7.5 L was pumped over each filter  
231 during a 2h period yielding a time series of near bottom SPOM supply and its variability over a period of  
232 48 hours.

233 *C/N analysis and isotope measurements*

234 Filters from the phytoplankton sampler were freeze-dried before further analysis. Half of each filter was  
235 used for phytopigment analysis and a ¼ section of each filter was used for analyzing organic carbon,  
236 nitrogen, and their stable isotope ratios. The filters, used for carbon analysis, were decarbonized by  
237 vapor of concentrated hydrochloric acid (2 M HCl supra) prior to analyses. Filters were transferred into  
238 pressed tin capsules (12x5 mm, Elemental Microanalysis) and  $\delta^{15}\text{N}$ ,  $\delta^{13}\text{C}$  and total weight percent of  
239 organic carbon and nitrogen were analyzed by a Delta V Advantage isotope ratio MS coupled on line to  
240 an Elemental Analyzer (Flash 2000 EA-IRMS) by a Conflo IV (Thermo Fisher Scientific Inc.). The used  
241 reference gas was purified atmospheric N<sub>2</sub>. As a standard for  $\delta^{13}\text{C}$  benzoic acid and acetanilide was used,  
242 for  $\delta^{15}\text{N}$  acetanilide, urea and casein was used. For  $\delta^{13}\text{C}$  analysis a high signal method was exercised  
243 including a 70% dilution. Values are reported relative to v-pdb and the atmosphere respectively.  
244 Precision and accuracy based on replicate analyses and comparing international standards for  $\delta^{13}\text{C}$  and  
245  $\delta^{15}\text{N}$  was  $\pm 0.15\text{‰}$ . The C/N ratio is based on the weight ratios between TOC and N.

246 *Phytopigments*

247 Phytopigments were measured by reverse-phase high-performance liquid chromatography (RP-HPLC,  
248 Waters Acuity UPLC) with a gradient based on the method published by (Kraay et al., 1992). For each  
249 sample half of a GF/F filter was used and freeze-dried before extraction. Pigments were extracted using  
250 95% methanol and sonification. All steps were performed in a dark and cooled environment. Pigments  
251 were identified by means of their absorption spectrum, fluorescence and the elution time. Identification  
252 and quantification took place as described by Tahey et al. (1994). The absorbance peak areas of  
253 chlorophyll- $\alpha$  were converted into concentrations using conversion factors determined with a certified  
254 standard. The  $\Sigma$ Phaeopigment/ Chlorophyll- $\alpha$  ratio gives an indication about the degradation status of

255 the organic material, since phaeopigments form as a result of bacterial or autolytic cell lysis and grazing  
256 activity (Welschmeyer and Lorenzen, 1985).

257 *2.2.5 Tidal analysis*

258 The barotropic (due to the sea level and pressure change) and baroclinic (internal 'free waves'  
259 propagating along the pycnoclines) tidal signals obtained by the Aquadopp (Nortek™) profiling current  
260 meter were analyzed from the bottom pressure and from the horizontal flow components recorded 6 m  
261 above the sea floor, using the harmonic analysis toolbox *t\_tide* (Pawlowicz et al., 2002). The data mean  
262 and trends were subtracted from the data before analysis.

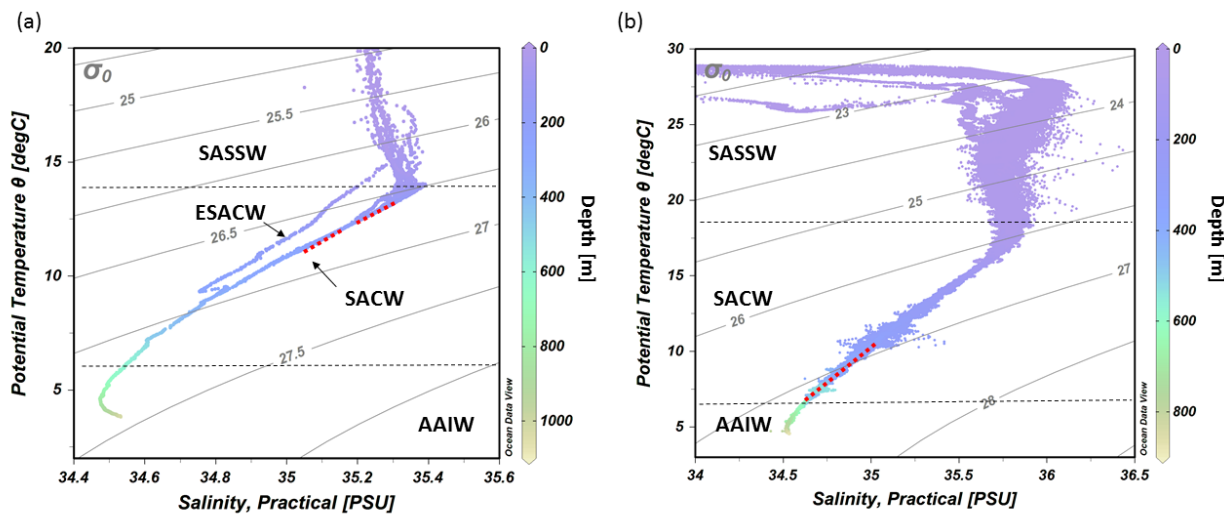
263 **3. Results**

264 **3.1 Water column properties**

265 *3.1.1 Namibian margin*

266 The hydrographic data obtained by CTD measurements along a downslope transect from the surface to  
267 1000 m water depth revealed distinct changes in temperature and salinity throughout the water  
268 column. These are ascribed to the different water masses in the study area (Fig. 3a). In the upper 85 m  
269 of the water column, temperatures were above 14 °C and salinities > 35.2, which corresponds to South  
270 Atlantic Subtropical Surface Water (SASSW). SACW was situated underneath the SASSW and reaches  
271 down to about 700 m, characterized by a temperature from 14-7 °C and a salinity from 35.4-34.5 (Fig.  
272 3a). A deep CTD cast about 130 km from the coastline recorded a water mass with the signature of  
273 ESACW, having a lower temperature ( $\Delta$  1.3 °C) and lower salinity ( $\Delta$  0.2) than SACW (in 200 m depth, not  
274 included in CTD transects of Fig. 4). Underneath these two central water masses Antarctic Intermediate

275 Water (AAIW) was found with a temperature  $<7$  °C.

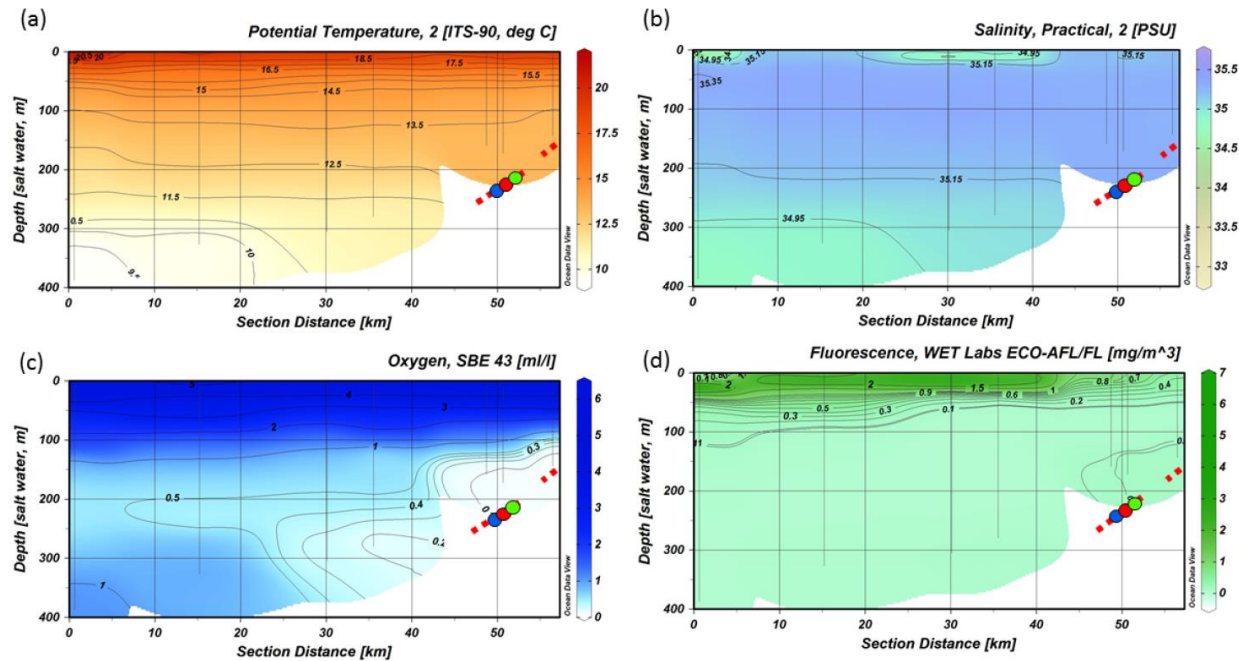


276

277 **Figure 3** TS-diagrams showing the different water masses being present at the (a) Namibian and (b) Angolan margins: South  
278 Atlantic Subtropical Surface Water (SASSW), South Atlantic Central Water (SACW) and Eastern South Atlantic Central water  
279 (ESACW), Antarctic Intermediate Water (AAIW) (data plotted using Ocean Data View v.4.7.8; <http://odv.awi.de>; Schlitzer, 2011).  
280 Red dotted line indicates the depth range of cold-water coral mound occurrence.

281 The CTD transect showed decreasing DO (dissolved oxygen) concentration from the surface ( $6 \text{ ml l}^{-1}$ )  
282 towards a minimum in 150-200 m depth ( $0 \text{ ml l}^{-1}$ ). Lowest values for  $\text{DO}_{\text{conc}}$  were found on the  
283 continental margin between 100-335 m water depth. The  $\text{DO}_{\text{conc}}$  in this pronounced OMZ ranged from  
284  $<1 \text{ ml l}^{-1}$  down to  $0 \text{ ml l}^{-1}$  ( $\triangleq 9-0\%$  saturation, respectively). The zone of low  $\text{DO}_{\text{conc}}$  ( $<1 \text{ ml l}^{-1}$ ) was  
285 stretching horizontally over the complete transect from about 50 towards at least 100 km offshore (Fig.  
286 4c). The upper boundary of the OMZ was relatively sharp compared to its lower limits and corresponded  
287 with the border between SASSW at the surface and SACW below.

288 Within the OMZ, a small increase in fluorescence ( $0.2 \text{ mg m}^{-3}$ ) was recorded, whereas fluorescence was  
289 otherwise not traceable below the surface layer (Fig. 4d). Within the surface layer highest surface  
290 fluorescence ( $>2 \text{ mg m}^{-3}$ ) was found  $\sim 40$  km offshore. Above the center of the OMZ fluorescence  
291 reached only up to  $0.4 \text{ mg m}^{-3}$ .



292

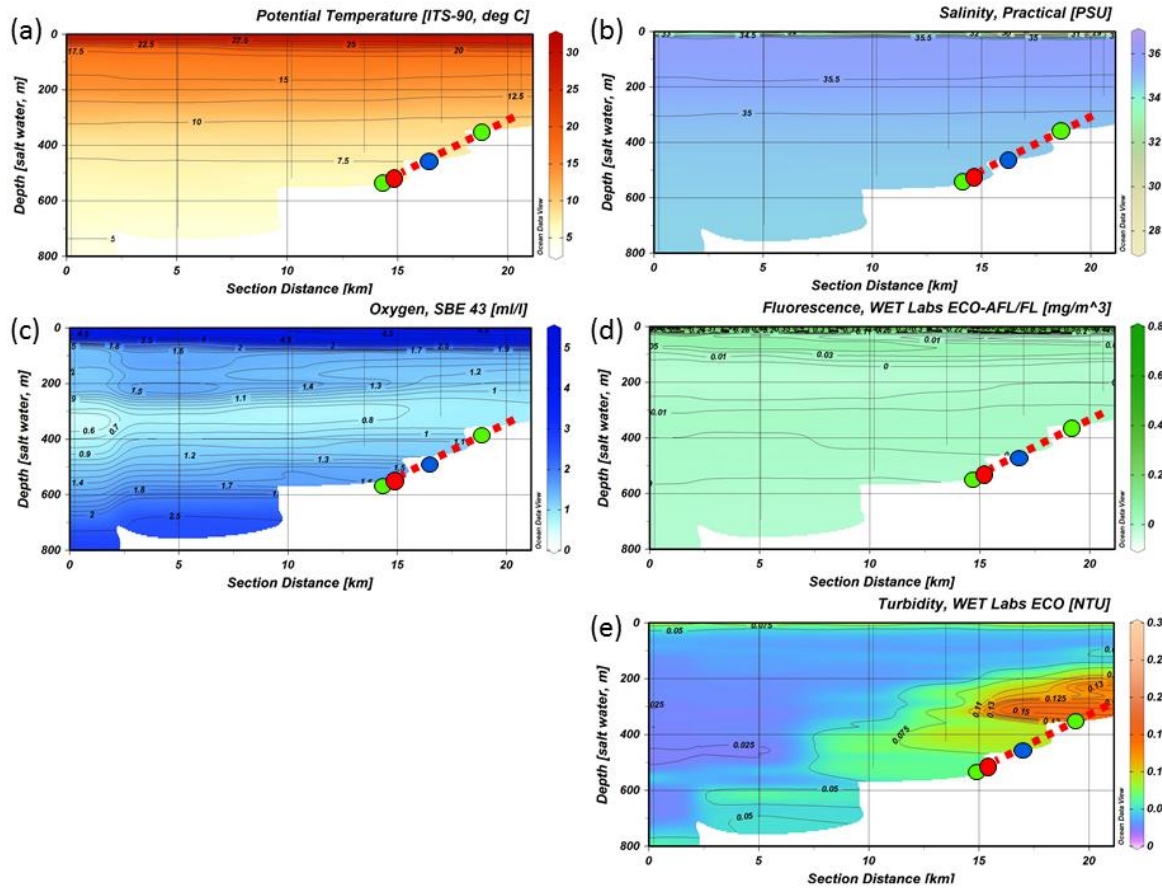
293 **Figure 4** CTD transect across the Namibian margin from west to east towards 50 km from the coastline. Data are presented for:  
294 (a) potential temperature ( $^{\circ}\text{C}$ ), (b) salinity (PSU), (c) dissolved oxygen concentrations ( $\text{ml l}^{-1}$ ), note the pronounced oxygen  
295 minimum zone (OMZ) between 100-335 m water depth, and (d) fluorescence ( $\text{mg m}^{-3}$ ) (data plotted using Ocean Data View  
296 v.4.7.8; <http://odv.awi.de>; Schlitzer, 2011). The occurrence of fossil CWC mounds is indicated by a red dashed line, colored dots  
297 indicate bottom lander deployments.

298 *3.1.2 Angolan margin*

299 The hydrographic data obtained by CTD measurements along a downslope transect from the surface to  
300 800 m water depth revealed distinct changes in temperature and salinity throughout the water column,  
301 related to four different water masses. At the surface a distinct shallow layer (>20 m) with a distinctly  
302 lower salinity (27.3-35.5) and higher temperature (29.5-27  $^{\circ}\text{C}$ , Fig. 3b) was observed. Below the surface  
303 layer, SASSW was found down to a depth of 70 m, characterized by a higher salinity (35.8). SACW was  
304 observed between 70-600 m, showing the expected linear relationship between temperature and  
305 salinity. Temperature and salinity decreased from 17.5  $^{\circ}\text{C}$ /35.8 to 7  $^{\circ}\text{C}$ /34.6. At 700 m depth AAIW was  
306 recorded, characterized by a low salinity (<34.4) and temperature (<7  $^{\circ}\text{C}$ , Fig. 3b).

307 The CTD transect showed a sharp decrease in the  $\text{DO}_{\text{conc}}$  underneath the SASSW from 5 to <2  $\text{ml l}^{-1}$  (Fig.  
308 5).  $\text{DO}_{\text{conc}}$  was further decreasing until a minimum of 0.6  $\text{ml l}^{-1}$  at 350 m and subsequently increasing to  
309 >3  $\text{ml l}^{-1}$  at 800 m depth. Lowest  $\text{DO}_{\text{conc}}$  were not found at the slope but 70 km offshore in the center of  
310 the zone of reduced  $\text{DO}_{\text{conc}}$  between 200-450 m water depth (<1  $\text{ml l}^{-1}$ ). Compared to the Namibian  
311 margin (see Fig. 4), the hypoxic layer was situated further offshore, slightly deeper and overall  $\text{DO}_{\text{conc}}$

312 were higher (compare Fig. 4c). Also, the boundaries of the hypoxic zone were not as sharp. Fluorescence  
 313 near the sea surface was generally low (around 0.2 with small maxima of  $0.78 \text{ mg m}^{-3}$ ) and not  
 314 detectable deeper than 150 m depth. A distinct zone of enhanced turbidity was observed on the  
 315 continental margin between 200-350 m water depth.



316

317 **Figure 5** CTD transect across the Angolan margin. Shown are data for (a) potential temperature ( $^{\circ}\text{C}$ ), (b) salinity (PSU), (c)  
 318 dissolved oxygen concentration ( $\text{ml l}^{-1}$ ), (d) fluorescence ( $\text{mg m}^{-3}$ ), (e) turbidity (NTU) (data plotted using Ocean Data View  
 319 v.4.7.8; <http://odv.awi.de>; Schlitzer, 2011). The depth occurrence of CWC mounds is marked by a red, dashed line, the lander  
 320 deployments are indicated by colored dots.

321 3.2 Near bottom environmental data

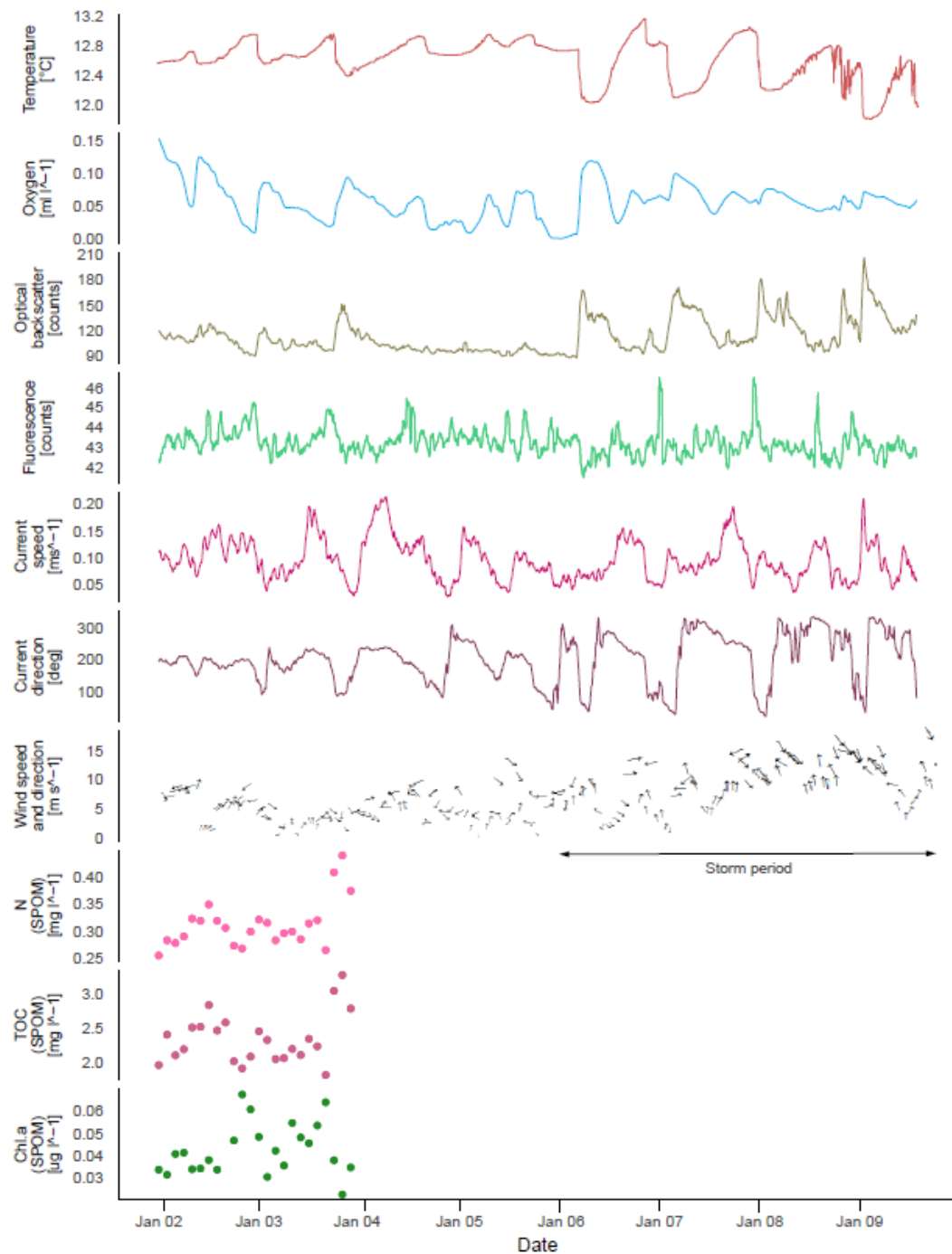
322 3.2.1 Namibian margin

323 Bottom temperature ranged from 11.8-13.2  $^{\circ}\text{C}$  during the deployment of the ALBEX lander (Table 2, Fig.  
 324 6) showing oscillating fluctuations with a maximum semidiurnal ( $\Delta T \sim 6\text{h}$ ) change of  $\sim \Delta 1 \text{ }^{\circ}\text{C}$  (on  
 325 9.1.2016). The  $\text{DO}_{\text{conc}}$  fluctuated between 0-0.15  $\text{ml l}^{-1}$  and was negatively correlated with temperature  
 326 ( $r=-0.39$ ,  $p<0.01$ ). Fluorescence ranged from 42-45 NTU during the deployment and was positively

327 correlated with temperature ( $r=0.38$ ,  $p<0.01$ ). Hence, both temperature and fluorescence were  
328 negatively correlated with  $\text{DO}_{\text{conc}}$  ( $r=-0.39$ ,  $p<0.01$ ) and turbidity (optical backscatter,  $r=-0.35$ ,  $p<0.01$ ).  
329 Turbidity was low until it increased especially during the second half of the deployment. During this  
330 period on the 6<sup>th</sup> of January wind speed increased from  $10 \text{ m s}^{-1}$  to a maximum of  $17 \text{ m s}^{-1}$  and remained  
331 high for the next six days. The wind direction changed from anticlockwise cyclonic rotation towards  
332 alongshore winds. During the strong wind period, colder water (correlation between wind speed and  
333 water temperature,  $r=-0.55$ ,  $p<0.01$ ), with a higher turbidity (correlation of wind speed and turbidity,  
334  $r=0.42$ ,  $p<0.01$ ) and on average higher  $\text{DO}_{\text{conc}}$  was present. The SLM lander recorded an average pH of  
335 8.01.

336 Maximum current speeds measured during the deployment period were  $0.21 \text{ m s}^{-1}$ , with average  
337 current speeds of  $0.09 \text{ m s}^{-1}$  (Table 2). The tidal cycle explained >80 % of the pressure fluctuations (Table  
338 3), with a semidiurnal signal, M2 (principal lunar semi-diurnal), generating an amplitude of >0.35 dbar  
339 and thus being the most important constituent. Before the 6<sup>th</sup> of January the current direction oscillated  
340 between SW and SE after which it changed into a dominating northern current direction (Fig. 6).

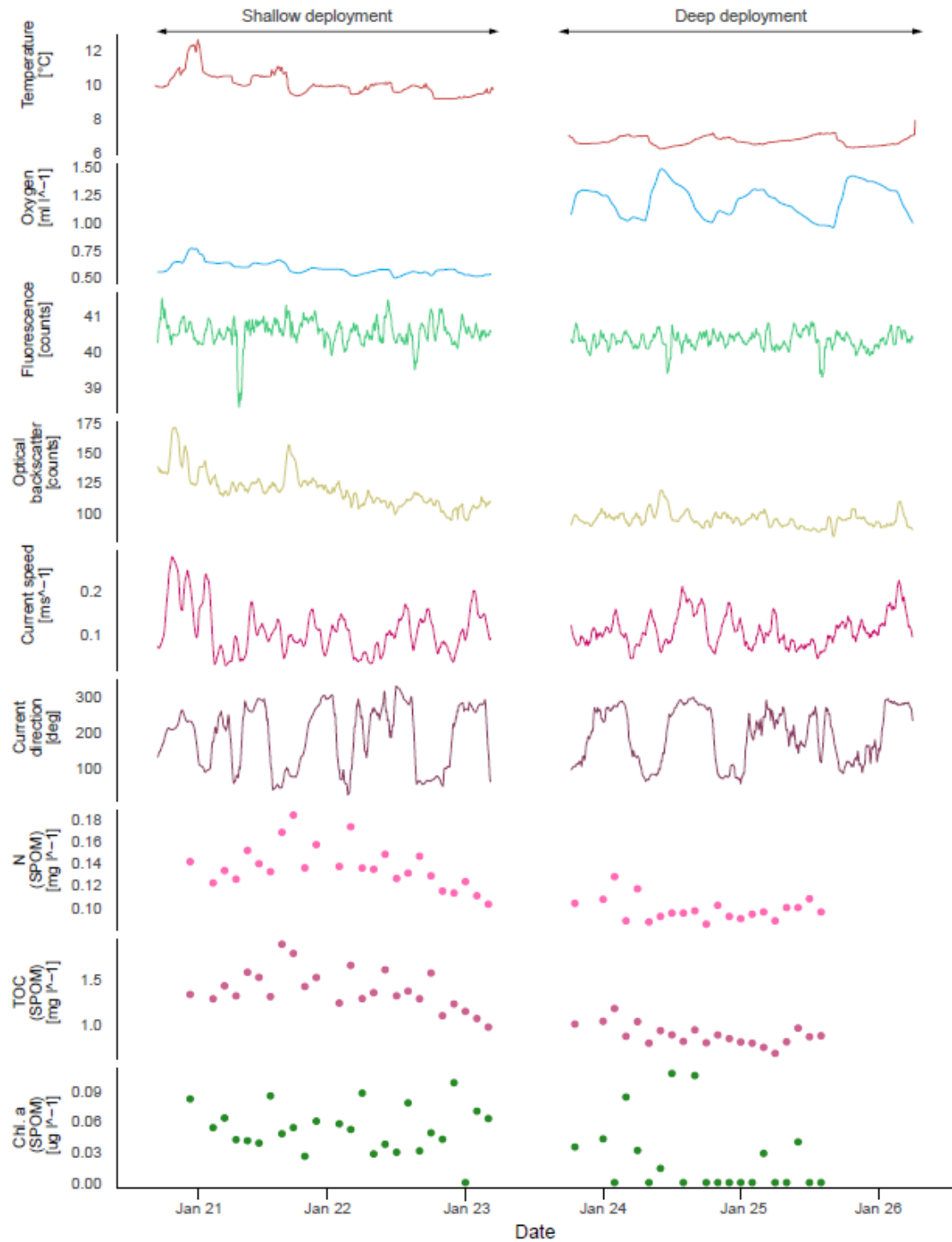
341 The observed fluctuations in bottom water temperature at the deployment site imply a vertical tidal  
342 movement of around 70 m. This was estimated by comparing the temperature change recorded by the  
343 lander to the respective temperature-depth gradient based on water column measurements (CTD site  
344 GeoB20553,  $12.58^\circ\text{C}$  at 245 m,  $12.93^\circ\text{C}$  at 179 m). Due to these vertical tidal movements, the oxygen  
345 depleted water from the core of the OMZ is regularly being replaced with somewhat colder and slightly  
346 more oxygenated water ( $\Delta$  up to  $0.2 \text{ ml l}^{-1}$ ).



347

348 **Figure 6** Data recorded by the ALBEX lander (210 m) at the Namibian margin in January 2016. Shown are data for temperature  
 349 ( $^{\circ}\text{C}$ ; red), dissolved oxygen concentrations ( $\text{ml l}^{-1}$ ; blue), optical backscatter (turbidity; moss green), fluorescence (counts per  
 350 second green), current speed ( $\text{m s}^{-1}$ ; pink), current direction (degree: 0-360°; dark red) as well as nitrogen ( $\text{mg l}^{-1}$ ; pink dots),  
 351 carbon ( $\text{mg l}^{-1}$ ; purple dots), and chlorophyll- $\alpha$  concentration ( $\mu\text{g l}^{-1}$ ; green dots) of SPOM collected during the first 48h by the  
 352 McLane pump. These data are supplemented by wind speed and direction (small black arrows) recorded concurrently to the  
 353 lander deployment by ship bound devices. Note that current directions changed from a generally south-poleward to an  
 354 equatorward direction when wind speed exceeded  $10 \text{ m s}^{-1}$  (stormy period indicated by black arrow).

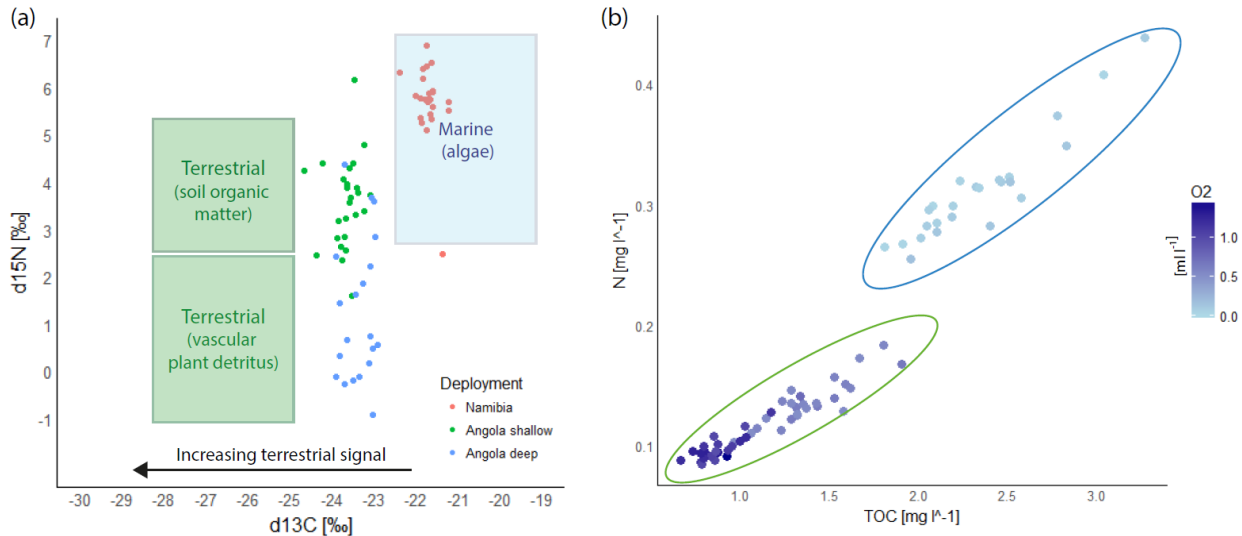
355 3.2.2 *Angolan margin*  
356 Mean bottom water temperatures was 6.73 °C at the deeper site (530 m) and 10.06 °C at the shallower  
357 site (340 m, Fig. 7, Table 2). The maximum semidiurnal ( $\Delta T \sim 6h$ ) temperature change was  $\Delta 1.60$  °C at  
358 the deepest site and  $\Delta 2.4$  °C at the shallow site (Fig. 7). DO<sub>conc</sub> at the deep site were a factor of two  
359 higher than those at the shallow site, i.e. 0.9-1.5 vs. 0.5-0.8 ml l<sup>-1</sup>respectively ( $\triangleq$  range between 4-14%  
360 saturation of both sites), whereas the range of diurnal fluctuations was much smaller compared to the  
361 shallow site. DO<sub>conc</sub> was negatively correlated with temperature at the deep site ( $r=-0.99$ ,  $p<0.01$ ) while  
362 positively correlated at the shallow site ( $r=0.91$ ,  $p<0.01$ ). Fluorescence was overall low during both  
363 deployments and showed only small fluctuations, being slightly higher at the shallow site (between 38.5  
364 and 41.5 NTU at both sites). Current speeds were relatively high (between 0-0.3 m s<sup>-1</sup>, average 0.1 m s<sup>-1</sup>)  
365 and positively correlated with temperature at the shallow site ( $r=0.31$ ,  $p<0.01$ ) and negatively correlated  
366 at the deep site ( $r=-0.22$ ,  $p<0.01$ ). Analysis of the tidal cycle showed, that it explained 29.8-54.9% of the  
367 horizontal current fluctuations. The M2 amplitude was 0.06-0.09 m s<sup>-1</sup> and was the most important  
368 signal (Table 3). A decrease in turbidity was observed during the deployment at the shallow station. This  
369 station was located directly below the turbidity maximum between 200-350 m depth as observed in the  
370 CTD transect (Fig.5). In contrast, a relative constant and low turbidity was observed for the deep  
371 deployment. Turbidity during both deployments was positively correlated to DO<sub>conc</sub> ( $r=0.47$ ,  $p<0.01$ ,  
372 shallow deployment and  $r=0.50$ ,  $p<0.01$ , deep deployment). The SLM lander recorded an average pH of  
373 8.12.  
374 The short-term temperature fluctuations imply a vertical tidal movement of around 130 m (12.9-9.1 °C  
375 measured by lander  $\triangleq$  218-349 m depth in CTD above lander at station GeoB20966).



376

377 **Figure 7** Lander data (ALBEX) recorded during at the shallow (~340 m water depth) and deep sites (~530 m water depth) off  
 378 Angola (January 2016). Shown are temperature (°C; red), dissolved oxygen concentration (ml l⁻¹; blue), fluorescence (counts per  
 379 second; green), optical backscatter (turbidity; yellow), current speed (m s⁻¹; pink) and current direction (degree: 0-360°; purple)  
 380 as well as nitrogen (mg l⁻¹; pink dots), carbon (mg l⁻¹; purple dots), and chlorophyll- $\alpha$  concentration (µg l⁻¹; green dots) of SPOM  
 381 collected during the both deployments by the McLane pump.

382 3.3 Suspended particulate matter  
383 3.3.1 Namibian margin  
384 The nitrogen (N) concentration of the SPOM measured on the filters of the McLane pump fluctuated  
385 between 0.25 and 0.45 mg l<sup>-1</sup> (Fig 8). The highest N concentration corresponded with a peak in turbidity  
386 ( $r=0.42$ ,  $p<0.01$ ). The  $\delta^{15}\text{N}$  values of the lander time series fluctuated between 5.1 and 6.9 with an  
387 average value of 5.7 ‰. Total Organic Carbon (TOC) showed a similar pattern as nitrogen, with relative  
388 concentrations ranging between 1.8-3.5 mg l<sup>-1</sup>. The  $\delta^{13}\text{C}$  value of the TOC increased during the surveyed  
389 time period from -22.39 to -21.24‰ with an average of -21.7 ‰ (Fig. 8a). The C/N ratio ranged from 8.5-  
390 6.8 and was on average 7.4 (Fig 8b). During periods of low temperature and more turbid conditions TOC  
391 and N as well as the  $\delta^{13}\text{C}$  values of the SPOM were higher.  
392 Chlorophyll- $\alpha$  concentrations of SPOM were on average 0.042  $\mu\text{g l}^{-1}$  and correlated with the record of  
393 the fluorescence ( $r=0.43$ ,  $p=0.04$ ). A six times higher amount of chlorophyll- $\alpha$  degradation products were  
394 found during the lander deployment (0.248  $\mu\text{g l}^{-1}$ ) compared to the amount of chlorophyll- $\alpha$ , giving a  
395  $\Sigma\text{Phaeopigment/Chlorophyll-}\alpha$  ratio of 6.5 (not shown). Additionally, carotenoids (0.08-0.12  $\mu\text{g l}^{-1}$ ) and  
396 fucoxanthin (0.22  $\mu\text{g l}^{-1}$ ) were found as major components of the pigment fraction, which are common in  
397 diatoms. Zeaxanthin, indicating the presence of prokaryotic cyanobacteria, was only observed in small  
398 quantities (0.066  $\mu\text{g l}^{-1}$ ).  
399 3.3.2 Angolan margin  
400 In general TOC and N concentrations of SPOM higher at the shallow compared to the deep site. Nitrogen  
401 concentrations varied around 0.14 mg l<sup>-1</sup> at 340 m and around 0.1 mg l<sup>-1</sup> at 530 m depth (Fig. 8b). The  
402  $\delta^{15}\text{N}$  values at the shallow site ranged from 1.6-6.2 ‰ (3.7 ‰ average) and were even lower deeper in  
403 the water column, viz. range 0.3-3.7 ‰ with an average of 1.4 ‰. The TOC concentrations were on  
404 average 1.43 mg l<sup>-1</sup> at 340 m and 0.9 mg l<sup>-1</sup> at 530 m, with corresponding  $\delta^{13}\text{C}$  values ranging between -  
405 23.0 and -24.2 (average of -23.6 ‰) at the shallow and between -22.9 and -23.9 (average -23.4 ‰) at  
406 the deep site.  
407 The chlorophyll- $\alpha$  concentrations of the SPOM collected by the McLane pump varied between 0.1 and  
408 0.02  $\mu\text{g l}^{-1}$ , with an average  $\Sigma\text{Phaeopigment/Chlorophyll-}\alpha$  ratio of 2.6 and 0.5 on the shallow and deep  
409 site, respectively. Phytopigments recorded by the shallow deployment included 0.3  $\mu\text{g l}^{-1}$  of fucoxanthin,  
410 while at the deep site only a concentration of 0.1  $\mu\text{g l}^{-1}$  was found. No zeaxanthin was recorded in the  
411 pigment fraction.



412

413 **Figure 8** Composite records of SPOM collected by the McLane pump of the ALBEX lander at the Namibian and Angolan margins  
 414 during all three deployments. (a)  $\delta^{15}\text{N}$  and  $\delta^{13}\text{C}$  isotopic values at the Namibian (red dots) and Angolan (blue and green dots)  
 415 margins. Indicated by the square boxes are common isotopic values of terrestrial and marine organic matter (Boutton 1991,  
 416 Holmes et al. 1997, Sigman et al. 2009). The relative contribution of terrestrial material (green boxes) is increasing with a more  
 417 negative  $\delta^{13}\text{C}$  value. (b) Total organic carbon (TOC) and nitrogen (N) concentration of the SPOM. Values of the Namibian margin  
 418 are marked by a blue circle (C/N ratio = 7.8), values of the Angolan margin are marked by a green circle (C/N ratio = 9.6).  
 419 Dissolved oxygen concentrations are included to show the higher nutrient concentrations in less oxygenated water.

## 4. Discussion

420 Even though the ecological-niche factor analysis of Davies et al. (2008) and Davies and Guinotte (2011)  
 421 predict *L. pertusa* to be absent along the oxygen-limited southwestern African margin, CWC mounds with  
 422 two distinct benthic ecosystems were found. The coral mounds on the Namibian shelf host no living CWCs,  
 423 instead dead coral framework covering the mounds was overgrown with fauna dominated by bryozoans  
 424 and sponges. Along the slope of the Angolan margin an extended coral mound area with thriving CWC  
 425 communities was encountered. Differences between the areas likely indicate that different  
 426 environmental conditions influence the faunal assemblages in both areas. The potential impact of the key  
 427 environmental factors will be discussed below.

### 429 4.1 Short-term vs long-term variations in environmental properties

430 On the Namibian margin, seasonality has a major impact on local-mid-depth oxygen concentration due  
 431 to the periodically varying influence of the Angola current and its associated low  $\text{DO}_{\text{conc}}$  (Chapman and  
 432 Shannon, 1987). The lowest  $\text{DO}_{\text{conc}}$  are expected from February to May when SACW is the dominating  
 433 water mass on the Namibian margin and the contribution of ESACW is smaller (Mohrholz et al., 2008).

434 Due to this seasonal pattern, the DO<sub>conc</sub> measured in this study (January; Fig. 4) most likely do not  
435 represent minimum concentrations, which are expected to occur in the following months, but  
436 nevertheless give a valuable impression about the extent of the OMZ (February to May; Mohrholz et al.,  
437 2014). Interestingly, we captured a flow reversal after the 6<sup>th</sup> of January from a southward to an  
438 equatorward current direction during high wind conditions on the Namibian margin (Fig. 6), leading to  
439 an intrusion of ESACW with higher DO<sub>conc</sub> ( $\Delta 0.007 \text{ ml l}^{-1}$  on average) and lower temperatures ( $\Delta 0.23 \text{ }^{\circ}\text{C}$   
440 on average, Fig. 5) than the SACW. This was leading to a temporal increase in the DO<sub>conc</sub>. This shows that  
441 variations in the local flow field have the capability to change water properties on relatively short time  
442 scales, which might provide an analogue to the water mass variability related to the different seasons  
443 (Mohrholz et al., 2008). Such relaxations are likely important for the survival of the abundant benthic  
444 fauna present on the relict coral mounds (Gibson et al. , 2003). Other seasonal changes, like riverine  
445 outflow do not have decisive impacts on the ecosystem since only relatively small rivers discharge from  
446 the Namibian margin. This is also reflected by the dominant marine isotopic signature of the isotopic  
447 ratios of  $\delta^{15}\text{N}$  and  $\delta^{13}\text{C}$  of the SPOM at the mound areas (Fig. 8, cf. Tyrrell and Lucas, 2002).

448 Flow reversals were not observed during the lander deployments on the Angolan margin, where winds  
449 are reported to be weak throughout the year providing more stable conditions (Shannon, 2001). Instead  
450 river outflow seems to exert a strong influence on the DO<sub>conc</sub> on the Angolan margin. The run-off of the  
451 Cuanza and Congo river reach their seasonal maximum in December and January (Kopte et al., 2017),  
452 intensifying upper water column stratification. This stratification is restricting vertical mixing and  
453 thereby limits ventilation of the oxygen depleted subsurface water masses. In addition rivers transport  
454 terrestrial organic matter to the margin, which is reflected by the isotopic signals of the SPOM (-1 to  
455 3‰; Montoya, 2007) which is well below the average isotopic ratio of the marine waters of 5.5 ‰  
456 (Meisel et al., 2011). Also  $\delta^{13}\text{C}$  values are in line with the  $\delta^{13}\text{C}$  values of terrestrial matter which is on  
457 average -27 ‰ in this area (Boutton, 1991; Mariotti et al., 1991). The C/N ratio of SPOM is higher  
458 compared to material from the Namibian margin, also confirming admixing of terrestrial matter (Perdue  
459 and Koprivnjak, 2007). This terrestrial matter contains suitable food sources as well as less suitable food  
460 sources, like carbon rich polymeric material (cellulose, hemicellulose and lignin) which cannot easily be  
461 taken up by marine organisms (Hedges and Oades, 1997). The combined effects of decreased vertical  
462 mixing and additional input of organic matter potentially result in the lowest DO<sub>conc</sub> of the year during  
463 the investigated time period (January), since the highest river outflow and therefore strongest  
464 stratification is expected during this period.

465 **4.2 Main stressors – Oxygen and temperature**

466 Environmental conditions marked by severe hypoxia and temporal anoxia (<0.17 ml l<sup>-1</sup>) likely explain the  
467 present-day absence of living CWCs along the Namibian margin. During the measurement period the  
468 DO<sub>conc</sub> off Namibia were considerably lower than thus far recorded minimum concentrations near living  
469 CWCs (1-1.3 ml l<sup>-1</sup>), which were found off Mauritania where only isolated living CWCs are found (Ramos  
470 et al., 2017). Age dating of the Namibian fossil coral framework showed that CWCs disappeared about 5  
471 ka BP, which coincides with an intensification in upwelling and therefore most likely a decline of DO<sub>conc</sub>  
472 (Tamborrino et al., accepted), supporting the assumption that the low DO<sub>conc</sub> are responsible for the  
473 demise of CWCs on the Namibian margin. Although no living corals were observed on the Namibian  
474 coral mounds, we observed a dense living community dominated by sponges and bryozoans (Hebbeln et  
475 al., 2017). Several sponge species have been reported to survive at extremely low DO<sub>conc</sub> within OMZs.  
476 For instance, along the lower boundary of the Peruvian OMZ sponges were found at DO<sub>conc</sub> as low as  
477 0.06-0.18 ml l<sup>-1</sup> (Mosch et al., 2012). Mills et al. (2018) recently found a sponge (*Tethya wilhelma*) to be  
478 physiologically almost insensitive to oxygen stress and to respire aerobically under low DO<sub>conc</sub> (0.02 ml l<sup>-1</sup>).  
479 Sponges can potentially stop their metabolic activity during unfavorable conditions and re-start their  
480 metabolism when some oxygen becomes available, for instance during diurnal irrigation of water with  
481 somewhat higher DO<sub>conc</sub>. The existence of a living sponge community off Namibia might therefore be  
482 explained by the diurnal tides occasionally flushing the sponges with more oxic water enabling them to  
483 metabolize, when food availability is highest (Figs. 6). Increased biomass and abundances in these  
484 temporary hypoxic-anoxic transition zones were already observed for macro- and mega-fauna in other  
485 OMZs and is referred to as the “edge effect” (Mullins et al., 1985; Levin et al., 1991; Sanders, 1969). It is  
486 very likely that this mechanism plays a role for the benthic communities on the Namibian as well as the  
487 Angolan margin.

488 Along the Angolan margin low oxygen concentrations apparently do not restrict the proliferation of  
489 thriving CWC reefs even though DO<sub>conc</sub> are considered hypoxic (0.5-1.5 ml l<sup>-1</sup>). The DO<sub>conc</sub> measured off  
490 Angola are well below the lower DO<sub>conc</sub> limits for *L. pertusa* based on laboratory experiments and earlier  
491 field observations (Schroeder, 2002; Brooke and Ross, 2014). The DO<sub>conc</sub> encountered at the shallow  
492 mound sites (<0.8 ml l<sup>-1</sup>) are even below the so far lowest limits known for single CWC colonies from the  
493 Mauritanian margin (Ramos et al., 2017b). Since in the present study, measured DO<sub>conc</sub> were even lower  
494 than the earlier established lower limits this could suggest a much higher tolerance of *L. pertusa* to low  
495 oxygen levels as low as 0.5 ml l<sup>-1</sup> at least in a limited time-period (4% O<sub>2</sub> saturation)

496 In addition to oxygen stress, heat stress is expected to put additional pressure on CWCs. Temperatures at  
497 the CWC mounds off Angola ranged from 6.4-12.6 °C, with the upper limit being close to reported  
498 maximum temperatures (~12-14.9 °C; Davies and Guinotte 2011) and are hence expected to impair the  
499 ability of CWCs to form mounds (see Wienberg and Titschack 2017). The CWCs were also occurring outside  
500 of the expected density envelope of 27.35-27.65 kg m<sup>-3</sup> in densities well below 27 kg m<sup>-3</sup> (Fig. 3, Dullo et  
501 al., 2008). In most aquatic invertebrates respiration rates roughly double with every 10 °C increase ( $Q_{10}$   
502 temperature coefficient = 2-3, e.g. Coma 2002), which at the same time doubles energy demand. Dodds  
503 et al. (2007) found a doubling of the respiration rate of *L. pertusa* with an increase at ambient temperature  
504 of only 2 °C (viz.  $Q_{10} = 7-8$ ). This would limit the survival of *L. pertusa* at high temperatures to areas where  
505 the increased demand in energy (due to increased respiration) can be compensated by high food  
506 availability. Higher respiration rates also imply that enough oxygen needs to be available for the increased  
507 respiration. However this creates a negative feedback, since with increased food availability and higher  
508 temperatures the oxygen concentration will decrease due to bacterial decomposition of organic  
509 substances.

510 Survival of *L. pertusa* under hypoxic conditions along the shallow Angolan CWC areas is probably positively  
511 influenced by the fact that periods of highest temperatures coincide with highest DO<sub>conc</sub> during the tidal  
512 cycle. Probably here the increase of one stressor is compensated by a reduction of another stressor. On  
513 the Namibian margin and the deeper Angolan mound sites the opposite pattern was found, with highest  
514 temperatures during lowest DO<sub>conc</sub>. However, at the deeper Angolan mound sites DO<sub>conc</sub> are higher and  
515 temperatures more within a suitable range compared to the shallow sites (0.9-1.5 ml l<sup>-1</sup>, 6.4-8 °C, Fig. 7).  
516 Additionally it was shown by ex situ experiments that *L. pertusa* is able to survive periods of hypoxic  
517 conditions similar to those found along the Angolan margin for several days, which could be crucial in  
518 periods of most adverse conditions (Dodds et al., 2007).

### 519 **4.3 Food supply**

520 As mentioned above, environmental stress like high temperature or low DO<sub>conc</sub> results in a loss of energy  
521 (Odum, 1971; Sokolova et al., 2012), which needs to be balanced by an increased energy (food)  
522 availability. Food availability therefore plays a significant role for faunal abundance under hypoxia or  
523 unfavorable temperatures (Diaz and Rosenberg, 1995). Above, we argued that survival of sponges and  
524 bryozoans on the relict mounds off Namibia and of CWCs and their associated fauna at the Angolan  
525 margin, may be partly due to a high input of high-quality organic matter, compensating the oxygen and  
526 thermal stresses. The importance of the food availability for CWCs was already suggested by Eisele et al.

527 (2011), who mechanistically linked CWC mound growth periods with enhanced surface water productivity  
528 and hence organic matter supply. Here we found evidence for high quality and quantity of SPOM in both  
529 areas indicated by high TOC and N concentrations (Figs. 6 and 7) in combination with a low C/N ratio (Fig.  
530 8), a low isotopic signature of  $\delta^{15}\text{N}$  and only slightly degraded pigments.

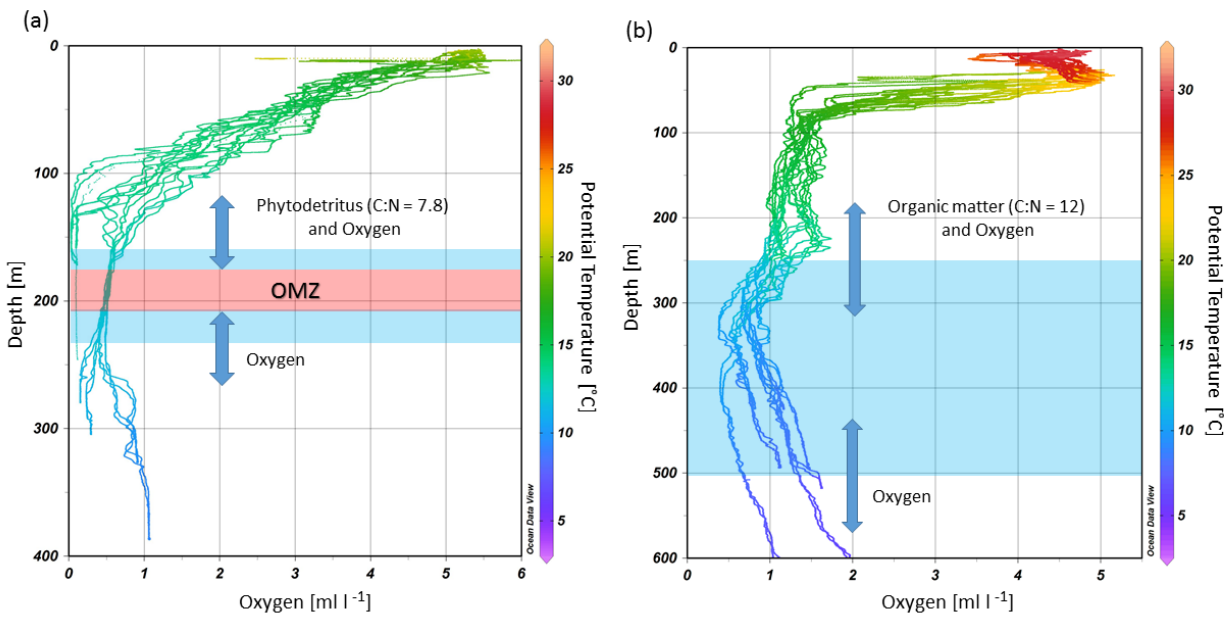
531 The Namibian margin is known for its upwelling cells, where phytoplankton growth is fueled by nutrients  
532 from deeper water layers producing high amounts of phytodetritus (Chapman and Shannon, 1985), which  
533 subsequently sinks down to the relict mounds on the slope. Benthic communities on the mounds off  
534 Namibia occur at relatively shallow depths, hence downward transport of SPOM from the surface waters  
535 is rapid and time for decomposition of the sinking particles in the water column is limited. The higher  
536 turbidity during lower current speeds provides additional evidence that the material settling from the  
537 surface is not transported away with the strong currents (Fig. 6).

538 At the Angolan coral mounds, SPOM appeared to have a signature corresponding to higher quality organic  
539 matter compared to off Namibia. The phytopigments were less degraded and the  $\delta^{15}\text{N}$ , TOC and N  
540 concentration of the SPOM was lower. However, here lower  $\delta^{15}\text{N}$  and higher  $\Sigma\text{phaeopigment}/\text{chlorophyll-}$   
541  $\alpha$  ratio are likely connected to a mixture with terrestrial OM input, which might constitute a less suitable  
542 food source for CWCs (Hedges and Oades, 1997). On the other hand the riverine input delivers dissolved  
543 nutrients, which can support the growth of phytoplankton, indirectly influencing food supply  
544 (Kiriakoulakis et al., 2007; Mienis et al., 2012). Moreover, the food quality at the shallow Angolan reefs  
545 was not coupled to periods of other environmental stressors and variations were relatively small during  
546 this study. At the Angolan margin we see a rather constant availability of SPOM. The slightly higher  
547 turbidity during periods of highest DO<sub>conc</sub>, (Fig. 7) suggest that the SPOM on the Angolan margin originates  
548 from the bottom nepheloid layer on the margin directly above the CWC mounds (Fig. 5e), which may  
549 represent a constant reservoir of fresh SPOM. This reservoir is likely fueled by directly sinking as well as  
550 advected organic matter from the surface ocean.

#### 551 **4.4 Tidal currents**

552 The semidiurnal tidal currents observed likely play a major role in the survival of benthic fauna on the SW  
553 African margin. On the Namibian margin internal waves deliver oxygen from the surface and deeper  
554 waters to the OMZ and thereby enabling benthic fauna on the fossil coral framework to survive in hypoxic  
555 conditions (Fig. 9a). At the same time these currents are likely responsible for the delivery of fresh SPOM  
556 from the surface productive zone to the communities on the margin, since they promote mixing between  
557 the water masses as well as they vertically displace the different water layers.

558 On the Angolan margin internal tides produce slightly faster currents and vertical excursions of up to 130  
 559 m which are twice as high as those on the Namibian margin. Similar to the Namibian margin these tidal  
 560 excursions deliver oxygen from shallower and deeper waters to the mound zone and thereby deliver  
 561 water with more suitable characteristics over the whole extend of the parts of the OMZ which otherwise  
 562 may harbor unsuitable properties for CWCs (Fig. 9b). Internal tides are also responsible for the formation  
 563 of a bottom nepheloid layer in 200-350 m depth (Fig. 5e). This layer is formed by trapping of organic  
 564 matter as well as bottom erosion due to turbulences created by the interaction of internal waves with the  
 565 margin topography, which intensifies near-bottom water movements. These internal waves are able to  
 566 move on the density gradient between the SACW and surface water mass, which can be located by  
 567 maxima of the buoyancy frequency  $N^2$  in 225 and 300 m depth. Tidal waves will be amplified due to a  
 568 critical match between the characteristic slope of the internal M2 tide and the bottom slope of the  
 569 Angolan margin, as is known from other continental slope regions (Dickson and McCave, 1986; Mienis et  
 570 al., 2007). As argued above, this turbid layer is likely important for the nutrition of the slightly deeper  
 571 situated CWC mounds, since vertical mixing is otherwise hindered by the strong stratification.



572

573 **Figure 9** Depth range of cold-water coral mound occurrences (blue shaded areas) at the (a) Namibian and (b) Angolan margins  
 574 in relation to the dissolved oxygen concentrations and potential temperature. Diurnal tides are delivering mainly phytodetritus  
 575 (shown in (a) and organic matter from the benthic nepheloid layer (shown in (b) as well as oxygen from above, and from below  
 576 to the mound sites (indicated by blue arrows, the length of which indicate the tidal ranges).

577 **5. Conclusions**

578 Different environmental properties explain the present conditions of the benthic communities on the  
579 southwestern African margin including temperature, DO<sub>conc</sub>, food supply and tidal movements. The  
580 DO<sub>conc</sub> likely defines the presence of the CWCs along the Namibian and the Angolan margin, whereas  
581 high temperatures constitute an additional stressor by increasing the respiration rate and therefore  
582 energy demand. On the Namibian margin, where DO<sub>conc</sub> dropped below 0.01 ml l<sup>-1</sup>, only fossil CWC  
583 mounds covered by a community dominated by sponges and bryozoans were found. This benthic  
584 community survives as it receives periodically waters with slightly higher DO<sub>conc</sub> (>0.03 ml l<sup>-1</sup>) due to  
585 regular tidal oscillations (semi diurnal) and erratic wind events (seasonal). At the same time, a high  
586 quality and quantity of SPOM sinking down from the surface water mass enables the epifaunal  
587 community to survive despite the oxygen stress and sustain its metabolic energy demand at the  
588 Namibian OMZ, while CWCs are not capable to withstand such extreme conditions. In contrast, thriving  
589 CWCs on the Angolan coral mounds were encountered despite the overall hypoxic conditions. The  
590 DO<sub>conc</sub> were slightly higher than those on the Namibian margin, but nevertheless below the lowest  
591 threshold that was so far reported for *L. pertusa* (Ramos et al., 2017; Davies et al., 2010; Davies et al.,  
592 2008). In combination with temperatures, close to the upper limits for *L. pertusa*, metabolic energy  
593 demand probably reached a maximum. High energy requirements might have been compensated by the  
594 general high availability of fresh resuspended SPOM. Fresh SPOM is accumulated on the Angolan margin  
595 just above the CWC area and is regularly supplied due to mixing by semidiurnal tidal currents, despite  
596 the restricted sinking of SPOM from the surface due to the strong stratification.

597 CWC and sponge communities are known to play an important role as a refuge, feeding ground and  
598 nursery for commercial fishes (Miller et al., 2012) and have a crucial role in the marine benthic pelagic  
599 coupling (Catalat et al., 2015). Their ecosystem services are threatened by the expected expansion of  
600 OMZs due to anthropogenic activities like rising nutrient loads and climate change (Breitburg et al.,  
601 2018). This study showed that benthic fauna is able to cope with low oxygen levels as long as sufficient  
602 high quality food is available. Further, reef associated sponge grounds, as encountered on the Namibian  
603 margin could play a crucial role in taking over the function of CWCs in marine carbon cycling as well as in  
604 providing a habitat for associated fauna, when conditions become unsuitable for CWCs.

605 **6. Data availability**

606 Data will be uploaded to Pangea after publication.

607

608 **7. Author contribution**

609 UH analyzed the physical and chemical data, wrote the manuscript and prepared the figures with  
610 contributions of all authors. FM, GD and ML designed the lander research. DH and CW led the cruise and  
611 wrote the initial cruise plan. FM and ML collected the data during the research cruise. WCD was  
612 responsible for water column measurements with the CTD. AF and ML provided habitat characteristics,  
613 including species identification of both CWC areas. KJ performed the tidal analysis and provided  
614 together with SF data of the SML lander. All authors contributed to the data interpretation and  
615 discussion of the manuscript.

616

617 **8. Competing interests**

618 The authors declare that they have no conflict of interest.

619

620 **9. Acknowledgements**

621 We thank the Captain of the *RV Meteor* cruise M122, Rainer Hammacher, his officers and crew, which  
622 contributed to the success of this cruise. We also like to thank the scientific and technical staff for their  
623 assistance during the cruise and the work in the laboratory. Greatly acknowledged are the efforts from  
624 the German Diplomatic Corps in the German Embassies in Windhoek and Luanda and in the Foreign  
625 Office in Berlin. We thank the German Science Foundation (DFG) for providing ship time on *RV Meteor*  
626 and for funding the ROV *Squid* operations to investigate the cold-water coral ecosystems off Angola and  
627 Namibia. This work was further supported through the DFG Research Center/ Cluster of Excellence  
628 “MARUM – The Ocean in the Earth System”. UH is funded by the SponGES project, which received  
629 funding from the European Union's Horizon 2020 research and innovation program under grant  
630 agreement No 679849. FM is supported by the Innovational Research Incentives Scheme of the  
631 Netherlands Organisation for Scientific Research (NWO-VIDI grant 016.161.360). GJR is supported by the  
632 Netherlands Earth System Science Centre (NESSC), financially supported by the Ministry of Education,  
633 Culture and Science (OCW). KJ is funded through the FATE project (Fate of cold-water coral reefs –  
634 identifying drivers of ecosystem change), supported by the Norwegian Research Council (NRC).

635 **10. References**

636 Boutton, T. W.: Stable carbon isotope ratios of natural materials: II. Atmospheric, terrestrial, marine, and  
637 freshwater environments, Carbon isotope techniques, 1, 173, 1991.

- 638 Breitburg, D., Levin, L. A., Oschlies, A., Grégoire, M., Chavez, F. P., Conley, D. J., Garçon, V., Gilbert, D.,  
639 Gutiérrez, D., and Isensee, K.: Declining oxygen in the global ocean and coastal waters, *Science*, 359,  
640 eaam7240, 2018.
- 641 Brooke, S., and Ross, S. W.: First observations of the cold-water coral *Lophelia pertusa* in mid-Atlantic  
642 canyons of the USA, *Deep Sea Research Part II: Topical Studies in Oceanography*, 104, 245-251, 2014.
- 643 Buhl-Mortensen, L., Vanreusel, A., Gooday, A. J., Levin, L. A., Priede, I. G., Buhl-Mortensen, P.,  
644 Gheerardyn, H., King, N. J., and Raes, M.: Biological structures as a source of habitat heterogeneity and  
645 biodiversity on the deep ocean margins, *Marine Ecology*, 31, 21-50, 2010.
- 646 Cairns, S. D.: Deep-water corals: an overview with special reference to diversity and distribution of deep-  
647 water scleractinian corals, *Bulletin of Marine Science*, 81, 311-322, 2007.
- 648 Carr, M.-E., and Kearns, E. J.: Production regimes in four Eastern Boundary Current systems, *Deep Sea*  
649 *Research Part II: Topical Studies in Oceanography*, 50, 3199-3221, 2003.
- 650 Cathalot, C., Van Oevelen, D., Cox, T. J., Kutt, T., Lavaleye, M., Duineveld, G., and Meysman, F. J.: Cold-  
651 water coral reefs and adjacent sponge grounds: Hotspots of benthic respiration and organic carbon  
652 cycling in the deep sea, *Frontiers in Marine Science*, 2, 37, 2015.
- 653 Cavan, E. L., Trimmer, M., Shelley, F., and Sanders, R.: Remineralization of particulate organic carbon in  
654 an ocean oxygen minimum zone, *Nature communications*, 8, 14847, 2017.
- 655 Chapman, P., and Shannon, L.: The Benguela ecosystem, Part II. Chemistry and related processes.  
656 *Oceanography and Marine Biology. An Annual Review*, 23, 183-251, 1985.
- 657 Chapman, P., and Shannon, L.: Seasonality in the oxygen minimum layers at the extremities of the  
658 Benguela system, *South African Journal of Marine Science*, 5, 85-94, 1987.
- 659 Coma, R.: Seasonality of in situ respiration rate in three temperate benthic suspension feeders,  
660 *Limnology and Oceanography*, 47, 324-331, 2002.
- 661 Costello, M. J., McCrea, M., Freiwald, A., Lundälv, T., Jonsson, L., Bett, B. J., van Weering, T. C., de Haas,  
662 H., Roberts, J. M., and Allen, D.: Role of cold-water *Lophelia pertusa* coral reefs as fish habitat in the NE  
663 Atlantic, in: *Cold-water corals and ecosystems*, Springer, Heidelberg, 771-805, 2005.
- 664 Davies, A. J., Wissak, M., Orr, J. C., and Roberts, J. M.: Predicting suitable habitat for the cold-water  
665 coral *Lophelia pertusa* (Scleractinia), *Deep Sea Research Part I: Oceanographic Research Papers*, 55,  
666 1048-1062, 2008.
- 667 Davies, A. J., Duineveld, G. C., Lavaleye, M. S., Bergman, M. J., van Haren, H., and Roberts, J. M.:  
668 Downwelling and deep-water bottom currents as food supply mechanisms to the cold-water coral  
669 *Lophelia pertusa* (Scleractinia) at the Mingulay Reef Complex, *Limnology and Oceanography*, 54, 620-  
670 629, 2009.
- 671 Davies, A. J., Duineveld, G. C., van Weering, T. C., Mienis, F., Quattrini, A. M., Seim, H. E., Bane, J. M., and  
672 Ross, S. W.: Short-term environmental variability in cold-water coral habitat at Viosca Knoll, Gulf of  
673 Mexico, *Deep Sea Research Part I: Oceanographic Research Papers*, 57, 199-212, 2010.
- 674 Davies, A. J., and Guinotte, J. M.: Global habitat suitability for framework-forming cold-water corals, *PLoS*  
675 one, 6, e18483, 2011.
- 676 De Haas, H., Mienis, F., Frank, N., Richter, T. O., Steinacher, R., De Stigter, H., Van der Land, C., and Van  
677 Weering, T. C.: Morphology and sedimentology of (clustered) cold-water coral mounds at the south  
678 Rockall Trough margins, NE Atlantic Ocean, *Facies*, 55, 1-26, 2009.
- 679 Diaz, R. J., and Rosenberg, R.: Marine benthic hypoxia: a review of its ecological effects and the  
680 behavioural responses of benthic macrofauna, *Oceanography and Marine Biology. An Annual Review*,  
681 33, 245-203, 1995.
- 682 Dickson, R., and McCave, I.: Nepheloid layers on the continental slope west of Porcupine Bank, *Deep Sea*  
683 *Research Part A. Oceanographic Research Papers*, 33, 791-818, 1986.

- 684 Dodds, L., Roberts, J., Taylor, A., and Marubini, F.: Metabolic tolerance of the cold-water coral *Lophelia*  
685 *pertusa* (Scleractinia) to temperature and dissolved oxygen change, *Journal of Experimental Marine*  
686 *Biology and Ecology*, 349, 205-214, 2007.
- 687 Dodds, L., Black, K., Orr, H., and Roberts, J.: Lipid biomarkers reveal geographical differences in food  
688 supply to the cold-water coral *Lophelia pertusa* (Scleractinia), *Marine Ecology Progress Series*, 397, 113-  
689 124, 2009.
- 690 Duineveld, G. C., Lavaleye, M. S., Bergman, M. J., De Stigter, H., and Mienis, F.: Trophic structure of a  
691 cold-water coral mound community (Rockall Bank, NE Atlantic) in relation to the near-bottom particle  
692 supply and current regime, *Bulletin of Marine Science*, 81, 449-467, 2007.
- 693 Dullo, W.-C., Flögel, S., and Rüggeberg, A.: Cold-water coral growth in relation to the hydrography of the  
694 Celtic and Nordic European continental margin, *Marine Ecology Progress Series*, 371, 165-176, 2008.
- 695 Eisele, M., Frank, N., Wienberg, C., Hebbeln, D., Correa, M. L., Douville, E., and Freiwald, A.: Productivity  
696 controlled cold-water coral growth periods during the last glacial off Mauritania, *Marine Geology*, 280,  
697 143-149, 2011.
- 698 Fink, H. G., Wienberg, C., Hebbeln, D., McGregor, H. V., Schmiedl, G., Taviani, M., and Freiwald, A.:  
699 Oxygen control on Holocene cold-water coral development in the eastern Mediterranean Sea, *Deep Sea*  
700 *Research Part I: Oceanographic Research Papers*, 62, 89-96, 2012.
- 701 Flögel, S., Dullo, W.-C., Pfannkuche, O., Kiriakoulakis, K., and Rüggeberg, A.: Geochemical and physical  
702 constraints for the occurrence of living cold-water corals, *Deep Sea Research Part II: Topical Studies in*  
703 *Oceanography*, 99, 19-26, 2014.
- 704 Frederiksen, R., Jensen, A., and Westerberg, H.: The distribution of the scleractinian coral *Lophelia*  
705 *pertusa* around the Faroe Islands and the relation to internal tidal mixing, *Sarsia*, 77, 157-171, 1992.
- 706 Freiwald, A.: Reef-forming cold-water corals, in: *Ocean margin systems*, Springer, 365-385, 2002.
- 707 Freiwald, A., Fossa, J. H., Grehan, A., Koslow, T., and Roberts, J. M.: Cold water coral reefs: out of sight-  
708 no longer out of mind, 2004.
- 709 Freiwald, A., Beuck, L., Rüggeberg, A., Taviani, M., Hebbeln, D., and Participants, R. V. M. C. M.-. The  
710 white coral community in the central Mediterranean Sea revealed by ROV surveys, *Oceanography*, 22,  
711 58-74, 2009.
- 712 Geissler, W., Schwenk, T., and Wintersteller, P.: Walvis Ridge Passive-Source Seismic Experiment  
713 (WALPASS) – Cruise No. MSM20/1 – January 06 – January 15, 2012 - Cape Town (South Africa) – Walvis  
714 Bay (Namibia), DFG-Senatskommission für Ozeanographie, MARIA S. MERIAN-Berichte, MSM20/1, 54  
715 pp., 2013.
- 716 Gori, A., Grover, R., Orejas, C., Sikorski, S., and Ferrier-Pagès, C.: Uptake of dissolved free amino acids by  
717 four cold-water coral species from the Mediterranean Sea, *Deep Sea Research Part II: Topical Studies in*  
718 *Oceanography*, 99, 42-50, 2014.
- 719 Grasmueck, M., Eberli, G. P., Viggiano, D. A., Correa, T., Rathwell, G., and Luo, J.: Autonomous  
720 underwater vehicle (AUV) mapping reveals coral mound distribution, morphology, and oceanography in  
721 deep water of the Straits of Florida, *Geophysical Research Letters*, 33, 2006.
- 722 Hebbeln, D., Wienberg, C., Wintersteller, P., Freiwald, A., Becker, M., Beuck, L., Dullo, W.-C., Eberli, G.,  
723 Glogowski, S., and Matos, L.: Environmental forcing of the Campeche cold-water coral province,  
724 southern Gulf of Mexico, *Biogeosciences (BG)*, 11, 1799-1815, 2014.
- 725 Hebbeln, D., Wienberg, C., Bender, M., Bergmann, F., Dehning, K., Dullo, W.-C., Eichstädtter, R., Flöter, S.,  
726 Freiwald, A., Gori, A., Haberkern, J., Hoffmann, L., João, F., Lavaleye, M., Leymann, T., Matsuyama, K.,  
727 Meyer-Schack, B., Mienis, F., Moçambique, I., Nowald, N., Orejas, C., Ramos Cordova, C., Saturov, D.,  
728 Seiter, C., Titschack, J., Vittori, V., Wefing, A.-M., Wilsenack, M., and Wintersteller, P.: ANNA Cold-Water  
729 Coral Ecosystems off Angola and Namibia - Cruise No. M122 - December 30, 2015 - January 31, 2016 -  
730 Walvis Bay (Namibia) - Walvis Bay (Namibia), METEOR-Berichte, M122 [https://doi.org/10.2312/cr\\_m122\\_2017](https://doi.org/10.2312/cr_m122_2017).

- 732 Hedges, J., and Oades, J.: Comparative organic geochemistries of soils and marine sediments, *Organic*  
733 *geochemistry*, 27, 319-361, 1997.
- 734 Henry, L.-A., and Roberts, J. M.: Biodiversity and ecological composition of macrobenthos on cold-water  
735 coral mounds and adjacent off-mound habitat in the bathyal Porcupine Seabight, NE Atlantic, *Deep Sea*  
736 *Research Part I: Oceanographic Research Papers*, 54, 654-672, 2007.
- 737 Henry, L.-A., and Roberts, J. M.: Global Biodiversity in Cold-Water Coral Reef Ecosystems, in: *Marine*  
738 *Animal Forests*, Springer, 235-256, 2017.
- 739 Hutchings, L., Van der Lingen, C., Shannon, L., Crawford, R., Verheyen, H., Bartholomae, C., Van der Plas,  
740 A., Louw, D., Kreiner, A., and Ostrowski, M.: The Benguela Current: An ecosystem of four components,  
741 *Progress in Oceanography*, 83, 15-32, 2009.
- 742 Junker, T., Mohrholz, V., Siegfried, L., and van der Plas, A.: Seasonal to interannual variability of water  
743 mass characteristics and currents on the Namibian shelf, *Journal of Marine Systems*, 165, 36-46, 2017.
- 744 Karstensen, J., Stramma, L., and Visbeck, M.: Oxygen minimum zones in the eastern tropical Atlantic and  
745 Pacific oceans, *Progress in Oceanography*, 77, 331-350, 2008.
- 746 Kiriakoulakis, K., Fisher, E., Wolff, G. A., Freiwald, A., Grehan, A., and Roberts, J. M.: Lipids and nitrogen  
747 isotopes of two deep-water corals from the North-East Atlantic: initial results and implications for their  
748 nutrition, in: *Cold-water corals and ecosystems*, edited by: Freiwald, A. a. R., J.M. (eds.), Springer,  
749 Heidelberg, 715-729, 2005.
- 750 Kiriakoulakis, K., Freiwald, A., Fisher, E., and Wolff, G.: Organic matter quality and supply to deep-water  
751 coral/mound systems of the NW European Continental Margin, *International Journal of Earth Sciences*,  
752 96, 159-170, 2007.
- 753 Kopte, R., Brandt, P., Dengler, M., Tchipalanga, P., Macuéria, M., and Ostrowski, M.: The Angola Current:  
754 Flow and hydrographic characteristics as observed at 11° S, *Journal of Geophysical Research: Oceans*,  
755 122, 1177-1189, 2017.
- 756 Kostianoy, A., and Lutjeharms, J.: Atmospheric effects in the Angola-Benguela frontal zone, *Journal of*  
757 *Geophysical Research: Oceans*, 104, 20963-20970, 1999.
- 758 Kraay, G. W., Zapata, M., and Veldhuis, M. J.: Separation of Chlorophylls c1c2, and c3 of marine  
759 Phytoplankton by Reverse Phase C18 high Performance liquid Chromatography 1, *Journal of Phycology*,  
760 28, 708-712, 1992.
- 761 Le Guilloux, E., Olu, K., Bourillet, J.-F., Savoye, B., Iglesias, S., and Sibuet, M.: First observations of deep-  
762 sea coral reefs along the Angola margin, *Deep Sea Research Part II: Topical Studies in Oceanography*, 56,  
763 2394-2403, 2009.
- 764 Levin, L. A., Huggett, C. L., and Wishner, K. F.: Control of deep-sea benthic community structure by  
765 oxygen and organic-matter gradients in the eastern Pacific Ocean, *Journal of Marine Research*, 49, 763-  
766 800, 1991.
- 767 Lutjeharms, J., and Stockton, P.: Kinematics of the upwelling front off southern Africa, *South African*  
768 *Journal of Marine Science*, 5, 35-49, 1987.
- 769 Mariotti, A., Gadel, F., and Giresse, P.: Carbon isotope composition and geochemistry of particulate  
770 organic matter in the Congo River (Central Africa): application to the study of Quaternary sediments off  
771 the mouth of the river, *Chemical Geology: Isotope Geoscience Section*, 86, 345-357, 1991.
- 772 Meisel, S., Struck, U., and Emeis, K. C.: Nutrient dynamics and oceanographic features in the central  
773 Namibian upwelling region as reflected in  $\delta^{15}\text{N}$ -signals of suspended matter and surface sediments,  
774 *Fossil Record*, 14, 153-169, 2011.
- 775 Mienis, F., De Stigter, H., White, M., Duineveld, G., De Haas, H., and Van Weering, T.: Hydrodynamic  
776 controls on cold-water coral growth and carbonate-mound development at the SW and SE Rockall  
777 Trough Margin, NE Atlantic Ocean, *Deep Sea Research Part I: Oceanographic Research Papers*, 54, 1655-  
778 1674, 2007.

- 779 Mienis, F., De Stigter, H., De Haas, H., and Van Weering, T.: Near-bed particle deposition and  
780 resuspension in a cold-water coral mound area at the Southwest Rockall Trough margin, NE Atlantic,  
781 Deep Sea Research Part I: Oceanographic Research Papers, 56, 1026-1038, 2009.
- 782 Mienis, F., Duineveld, G., Davies, A., Ross, S., Seim, H., Bane, J., and Van Weering, T.: The influence of  
783 near-bed hydrodynamic conditions on cold-water corals in the Viosca Knoll area, Gulf of Mexico, Deep  
784 Sea Research Part I: Oceanographic Research Papers, 60, 32-45, 2012.
- 785 Mienis, F., Duineveld, G., Davies, A., Lavaleye, M., Ross, S., Seim, H., Bane, J., Van Haren, H., Bergman,  
786 M., and De Haas, H.: Cold-water coral growth under extreme environmental conditions, the Cape  
787 Lookout area, NW Atlantic, Biogeosciences, 11, 2543, 2014.
- 788 Miller, R. J., Hocevar, J., Stone, R. P., and Fedorov, D. V.: Structure-forming corals and sponges and their  
789 use as fish habitat in Bering Sea submarine canyons, PLoS One, 7, e33885, 2012.
- 790 Mills, D. B., Francis, W. R., Vargas, S., Larsen, M., Elemans, C. P., Canfield, D. E., and Wörheide, G.: The  
791 last common ancestor of animals lacked the HIF pathway and resired in low-oxygen environments,  
792 eLife, 7, e31176, 2018.
- 793 Mohrholz, V., Bartholomae, C., Van der Plas, A., and Lass, H.: The seasonal variability of the northern  
794 Benguela undercurrent and its relation to the oxygen budget on the shelf, Continental Shelf Research,  
795 28, 424-441, 2008.
- 796 Mohrholz, V., Eggert, A., Junker, T., Nausch, G., Ohde, T., and Schmidt, M.: Cross shelf hydrographic and  
797 hydrochemical conditions and their short term variability at the northern Benguela during a normal  
798 upwelling season, Journal of Marine Systems, 140, 92-110, 2014.
- 799 Montoya, J. P.: Natural abundance of  $^{15}\text{N}$  in marine planktonic ecosystems, Stable isotopes in Ecology  
800 and Environmental Science, 176, 2007.
- 801 Mortensen, P. B., Hovland, T., Fosså, J. H., and Furevik, D. M.: Distribution, abundance and size of  
802 *Lophelia pertusa* coral reefs in mid-Norway in relation to seabed characteristics, Journal of the Marine  
803 Biological Association of the United Kingdom, 81, 581-597, 2001.
- 804 Mosch, T., Sommer, S., Dengler, M., Noffke, A., Bohlen, L., Pfannkuche, O., Liebetrau, V., and Wallmann,  
805 K.: Factors influencing the distribution of epibenthic megafauna across the Peruvian oxygen minimum  
806 zone, Deep Sea Research Part I: Oceanographic Research Papers, 68, 123-135, 2012.
- 807 Mueller, C., Larsson, A., Veugel, B., Middelburg, J., and Van Oevelen, D.: Opportunistic feeding on  
808 various organic food sources by the cold-water coral *Lophelia pertusa*, Biogeosciences, 11, 123-133,  
809 2014.
- 810 Mullins, H. T., Thompson, J. B., McDougall, K., and Vercoutere, T. L.: Oxygen-minimum zone edge effects:  
811 evidence from the central California coastal upwelling system, Geology, 13, 491-494, 1985.
- 812 Odum, H. T.: Environment, power and society, New York, USA, Wiley-Interscience, 1971.
- 813 Oevelen, D. v., Duineveld, G., Lavaleye, M., Mienis, F., Soetaert, K., and Heip, C. H.: The cold-water coral  
814 community as hotspot of carbon cycling on continental margins: A food-web analysis from Rockall Bank  
815 (northeast Atlantic), Limnology and Oceanography, 54, 1829-1844, 2009.
- 816 Perdue, E. M., and Koprivnjak, J.-F.: Using the C/N ratio to estimate terrigenous inputs of organic matter  
817 to aquatic environments, Estuarine, Coastal and Shelf Science, 73, 65-72, 2007.
- 818 Pichevin, L., Bertrand, P., Boussafir, M., and Disnar, J.-R.: Organic matter accumulation and preservation  
819 controls in a deep sea modern environment: an example from Namibian slope sediments, Organic  
820 Geochemistry, 35, 543-559, 2004.
- 821 Poole, R., and Tomczak, M.: Optimum multiparameter analysis of the water mass structure in the  
822 Atlantic Ocean thermocline, Deep Sea Research Part I: Oceanographic Research Papers, 46, 1895-1921,  
823 1999.
- 824 Rae, C. D.: A demonstration of the hydrographic partition of the Benguela upwelling ecosystem at  $26^{\circ}$   
825  $40^{\circ}\text{S}$ , African Journal of Marine Science, 27, 617-628, 2005.

- 826 Ramos, A., Sanz, J. L., Ramil, F., Agudo, L. M., and Presas-Navarro, C.: The Giant Cold-Water Coral  
827 Mounds Barrier Off Mauritania, in: Deep-Sea Ecosystems Off Mauritania, edited by: Ramos, A., Ramil, F.,  
828 Sanz, JL (Eds.), Springer, 481-525, 2017.
- 829 Roberts, J. M., Wheeler, A. J., and Freiwald, A.: Reefs of the deep: the biology and geology of cold-water  
830 coral ecosystems, *Science*, 312, 543-547, 2006.
- 831 Ruhl, H. A.: Community change in the variable resource habitat of the abyssal northeast Pacific, *Ecology*,  
832 89, 991-1000, 2008.
- 833 Sanders, H.: Benthic marine diversity and the stability-time hypothesis, *Brookhaven Symposia in Biology*,  
834 1969, 71-81,
- 835 Schlitzer, R.: Ocean Data View. <http://www.awi.de/odv>, 2011.
- 836 Schroeder, W.: Observations of *Lophelia pertusa* and the surficial geology at a deep-water site in the  
837 northeastern Gulf of Mexico, *Hydrobiologia*, 471, 29-33, 2002.
- 838 Shannon, L., Boyd, A., Brundrit, G., and Taunton-Clark, J.: On the existence of an El Niño-type  
839 phenomenon in the Benguela system, *Journal of Marine Research*, 44, 495-520, 1986.
- 840 Shannon, L., Agenbag, J., and Buys, M.: Large-and mesoscale features of the Angola-Benguela front,  
841 *South African Journal of Marine Science*, 5, 11-34, 1987.
- 842 Shannon, L., and Nelson, G.: The Benguela: large scale features and processes and system variability, in:  
843 *The South Atlantic*, Springer, Berlin, Heidelberg, 163-210, 1996.
- 844 Shannon, L.: Benguela Current, *Ocean Currents: A Derivative of Encyclopedia of Ocean Sciences*, 23-34,  
845 2001.
- 846 Sokolova, I. M., Frederich, M., Bagwe, R., Lannig, G., and Sukhotin, A. A.: Energy homeostasis as an  
847 integrative tool for assessing limits of environmental stress tolerance in aquatic invertebrates, *Marine  
848 Environmental Research*, 79, 1-15, 2012.
- 849 Tahey, T., Duineveld, G., Berghuis, E., and Helder, W.: Relation between sediment-water fluxes of  
850 oxygen and silicate and faunal abundance at continental shelf, slope and deep-water stations in the  
851 northwest Mediterranean, *Marine Ecology Progress Series*, 119-130, 1994.
- 852 Tamborrino, L., Wienberg, C., Titschack, J., Wintersteller, P., Mienis, F., Freiwald, A., Orejas, C., Dullo,  
853 W.-C., Haberkern, J., and Hebbeln, D.: Mid-Holocene extinction of cold-water corals on the Namibian  
854 shelf steered by the Benguela oxygen minimum zone, accepted.
- 855 Taviani, M., Remia, A., Corselli, C., Freiwald, A., Malinverno, E., Mastrototaro, F., Savini, A., and Tursi, A.:  
856 First geo-marine survey of living cold-water *Lophelia* reefs in the Ionian Sea (Mediterranean basin),  
857 *Facies*, 50, 409-417, 2005.
- 858 R Core Team, R. C.: R: A language and environment for statistical computing [Internet]. Vienna, Austria;  
859 2014. 2017.
- 860 Thiem, Ø., Ravagnan, E., Fosså, J. H., and Berntsen, J.: Food supply mechanisms for cold-water corals  
861 along a continental shelf edge, *Journal of Marine Systems*, 60, 207-219, 2006.
- 862 Titschack, J., Baum, D., De Pol-Holz, R., Lopez Correa, M., Forster, N., Flögel, S., Hebbeln, D., and  
863 Freiwald, A.: Aggradation and carbonate accumulation of Holocene Norwegian cold-water coral reefs,  
864 *Sedimentology*, 62, 1873-1898, 2015.
- 865 Tyrrell, T., and Lucas, M. I.: Geochemical evidence of denitrification in the Benguela upwelling system,  
866 *Continental Shelf Research*, 22, 2497-2511, 2002.
- 867 van Haren, H., Mienis, F., Duineveld, G. C., and Lavaleye, M. S.: High-resolution temperature  
868 observations of a trapped nonlinear diurnal tide influencing cold-water corals on the Logachev mounds,  
869 *Progress in Oceanography*, 125, 16-25, 2014.
- 870 van Soest, R. W., Cleary, D. F., de Kluijver, M. J., Lavaleye, M. S., Maier, C., and van Duyl, F. C.: Sponge  
871 diversity and community composition in Irish bathyal coral reefs, *Contributions to Zoology*, 76, 2007.

872 Welschmeyer, N. A., and Lorenzen, C. J.: Chlorophyll budgets: Zooplankton grazing and phytoplankton  
873 growth in a temperate fjord and the Central Pacific Gyre, Limnology and Oceanography, 30, 1-21,  
874 1985.  
875 Wheeler, A. J., Beyer, A., Freiwald, A., De Haas, H., Huvenne, V., Kozachenko, M., Olu-Le Roy, K., and  
876 Opderbecke, J.: Morphology and environment of cold-water coral carbonate mounds on the NW  
877 European margin, International Journal of Earth Sciences, 96, 37-56, 2007.  
878 White, M., Mohn, C., de Stigter, H., and Mottram, G.: Deep-water coral development as a function of  
879 hydrodynamics and surface productivity around the submarine banks of the Rockall Trough, NE Atlantic,  
880 in: Cold-water corals and ecosystems, edited by: A Freiwald, J. R., Springer, Heidelberg, 503-514, 2005.  
881 White, M., Wolff, G. A., Lundälv, T., Guihen, D., Kiriakoulakis, K., Lavaleye, M., and Duineveld, G.: A  
882 Freiwald, JM Roberts, Cold-water coral ecosystem (Tisler Reef, Norwegian Shelf) may be a hotspot for  
883 carbon cycling, Marine Ecology Progress Series, 465, 11-23, 2012.  
884 Wienberg, C., and Titschack, J.: Framework-forming scleractinian cold-water corals through space and  
885 time: a late Quaternary North Atlantic perspective, Ros-si S, Bramanti L, Gori A, Orejas C, Marine Animal  
886 Forests: the Ecology of Benthic Biodiversity Hotspots, Springer, 699-732 pp., 2017.  
887 Wienberg, C., Titschack, J., Freiwald, A., Frank, N., Lundälv, T., Taviani, M., Beuck, L., Schröder-Ritzrau,  
888 A., Krengel, T., and Hebbeln, D.: The giant Mauritanian cold-water coral mound province: Oxygen control  
889 on coral mound formation, Quaternary Science Reviews, 185, 135-152, 2018.  
890 Wilson, J.: 'Patch' development of the deep-water coral *Lophelia pertusa* (L.) on Rockall Bank, Journal of  
891 the Marine Biological Association of the United Kingdom, 59, 165-177, 1979.  
892 Zabel, M., Boetius, A., Emeis, K.-C., Ferdelman, T. G., and Spieß, V.: PROSA Process Studies in the Eastern  
893 South Atlantic – Cruise No. M76 – April 12 – August 24, 2008 – Cape Town (South Africa) – Walvis Bay  
894 (Namibia)., DFG Senatskommission für Ozeanographie, METEOR-Berichte, M76, 180 pp., 2012.

## 895 11. Figure captions

896 **Figure 1** (a) Overview map showing the research areas off Angola and Namibia (red squares) and main features of the surface  
897 water circulation (arrows) and frontal zone (dashed line) in the SE Atlantic as well as the two main rivers discharging at the  
898 Angolan margin. Detailed bathymetry maps of the Angolan (upper maps) and Namibian margins (lower maps) showing the  
899 position of (b) CTD transects (note the deep CTD cast down to 1000 m water depth conducted off Namibia) and (c) bottom  
900 lander deployments (red squares shown in b indicate the cutouts displayed in c).

901 **Figure 2** ROV images (copyright MARUM ROV SQUID, Bremen, Germany) showing the surface coverage of cold-water coral  
902 mounds discovered off Namibia (a, b) and Angola (c, d). Images were recorded and briefly described for their faunal  
903 composition during RV Meteor cruise M122 "ANNA" (see Hebbeln et al. 2017). (a) Sylvester mound, 225 m water depth. Dead  
904 coral framework entirely consisting of *L. pertusa*. The framework is intensely colonized by the yellow bryozoan *Metropriella* sp.,  
905 zoanthids, actinarians and sponges. Vagile fauna consists of asteroids and gobiid fishes (*Sufflogobius bibarbatus*) that hide  
906 between hollows underneath the coral framework. (b) Sylvester mound, 238 m water depth. Dense coral rubble (*L. pertusa*)  
907 heavily overgrown by *Metropriella* sp. and sponges. Note the decapod crab *Macropipus australis* (center of the image). (c)  
908 Valentine mound, 238 m water depth. Live *L. pertusa* colony being grazed by echinoids. Note the sponge *Aphrocallistes* sp. with  
909 its actinarian symbionts (right side of the image). (d) Buffalo mound, 345 m water depth. Living CWC reef observed on top of an  
910 Angolan coral mound. Many fishes are present around the reef (*Helicolenus dactylopterus*, *Gephyroberyx darwini*).

911 **Figure 3** TS-diagrams showing the different water masses being present at the (a) Namibian and (b) Angolan margins: South  
912 Atlantic Subtropical Surface Water (SASSW), South Atlantic Central Water (SACW) and Eastern South Atlantic Central water

913 (ESACW), Antarctic Intermediate Water (AAIW) (data plotted using Ocean Data View v.4.7.8; <http://odv.awi.de>; Schlitzer, 2011).  
914 Red dotted line indicates the depth range of cold-water coral mound occurrence.

915 **Figure 4** CTD transect across the Namibian margin. Shown are data for: (a) potential temperature (°C), (b) salinity (PSU), (c)  
916 dissolved oxygen concentrations (ml l<sup>-1</sup>), note the pronounced oxygen minimum zone (OMZ) between 100-335 m water depth,  
917 and d) fluorescence (mg m<sup>-3</sup>) (data plotted using Ocean Data View v.4.7.8; <http://odv.awi.de>; Schlitzer, 2011). The occurrence of  
918 fossil CWC mounds is indicated by a red dashed line, colored dots indicate bottom lander deployments.

919 **Figure 5** CTD transect across the Angolan margin. Shown are data for (a) potential temperature (°C), (b) salinity (PSU), (c)  
920 dissolved oxygen concentration (ml l<sup>-1</sup>), (d) fluorescence (mg m<sup>-3</sup>), (e) turbidity (NTU) (data plotted using Ocean Data View  
921 v.4.7.8; <http://odv.awi.de>; Schlitzer, 2011). The depth occurrence of CWC mounds is marked by a red, dashed line, the lander  
922 deployments are indicated by colored dots.

923 **Figure 6** Data recorded by the ALBEX lander (210 m) at the Namibian margin in January 2016. Shown are data for temperature  
924 (°C; red), dissolved oxygen concentrations (ml l<sup>-1</sup>; blue), optical backscatter (turbidity; moss green), fluorescence (counts per  
925 second green), current speed (m s<sup>-1</sup>; pink), current direction (degree: 0-360°; dark red) as well as nitrogen (mg l<sup>-1</sup>; pink dots),  
926 carbon (mg l<sup>-1</sup>; purple dots), and chlorophyll- $\alpha$  concentration ( $\mu$ g l<sup>-1</sup>; green dots) of SPOM collected during the first 48h by the  
927 McLane pump. These data are supplemented by wind speed and direction (small black arrows) recorded concurrently to the  
928 lander deployment by ship bound devices. Note that current directions changed from a generally south-poleward to an  
929 equatorward direction when wind speed exceeded 10 m s<sup>-1</sup> (stormy period indicated by black arrow).

930 **Figure 7** Lander data (ALBEX) recorded during the shallow (~340 m water depth) and deep deployments (~530 m water depth)  
931 off Angola (January 2016). Shown are temperature (°C; red), dissolved oxygen concentration (ml l<sup>-1</sup>; blue), fluorescence (counts  
932 per second; green), optical backscatter (turbidity; yellow), current speed (m s<sup>-1</sup>; pink) and current direction (degree: 0-360°;  
933 purple) as well as nitrogen (mg l<sup>-1</sup>; pink dots), carbon (mg l<sup>-1</sup>; purple dots), and chlorophyll- $\alpha$  concentration ( $\mu$ g l<sup>-1</sup>; green dots) of  
934 SPOM collected during the both deployments by the McLane pump.

935 **Figure 8** Composite records of SPOM collected by the McLane pump of the ALBEX lander at the Namibian and Angolan margins  
936 during all three deployments. (a)  $\delta^{15}\text{N}$  and  $\delta^{13}\text{C}$  isotopic values at the Namibian (red dots) and Angolan (blue and green dots)  
937 margins. Indicated by the square boxes are common isotopic values of terrestrial and marine organic matter (Boutton 1991,  
938 Holmes et al. 1997, Sigman et al. 2009). The relative contribution of terrestrial material (green boxes) is increasing with a more  
939 negative  $\delta^{13}\text{C}$  value. (b) Total organic carbon (TOC) and nitrogen (N) concentration of the SPOM. Values of the Namibian  
940 margin are marked by a blue circle (C/N ratio = 7.8), values of the Angolan margin are marked by a green circle (C/N ratio = 9.6).  
941 Dissolved oxygen concentrations are included to show the higher nutrient concentrations in less oxygenated water.

942 **Figure 9** Depth range of cold-water coral mound occurrences (blue shaded areas) at the (a) Namibian and (b) Angolan margins  
943 in relation to the dissolved oxygen concentrations and potential temperature. Diurnal tides are delivering mainly phytodetritus  
944 (shown in (a) and organic matter from the benthic nepheloid layer (shown in (b) as well as oxygen from above, and from below  
945 to the mound sites (indicated by blue arrows, the length of which indicate the tidal ranges).

946 **12. Tables**

947 **Table 1.** Metadata of lander deployments conducted during RV *Meteor* cruise M122 (ANNA) in January 2016. The deployment  
 948 sites are shown in Figure 1.

	Station no. (GeoB ID)	Area	Lander	Date	Latitude [S]	Longitude [E]	Depth [m]	Duration [days]	Devices
<b>Namibia</b>	20507-1	on-mound	ALBEX	01.- 09.01.16	20°44.03'	12°49.23'	210	7.8	+ particle pump
	20506-1	off-mound	SLM	01.- 16.01.16	20°43.93'	12°49.11'	230	12.5	
<b>Angola</b>	20921-1	off-mound	ALBEX	20.- 23.01.16	9°46.16'	12°45.96'	340	2.5	+ particle pump
	20940-1	off-mound	ALBEX	23.- 26.01.16	9°43.84'	12°42.15'	530	2.6	+ particle pump
	20915-2	off-mound	SLM	19.- 26.01.16	9°43.87'	12°43.87'	430	6.8	

949

950 **Table 2** Environmental properties at the Namibian and Angolan margins.

	Namibia	Angola
<b>Temperature [°C]</b>	11.8-13.2	6.73-12.9
<b>DO<sub>conc</sub> [ml l<sup>-1</sup>]</b>	0-0.15	0.5-1.5
<b>Fluorescence [NTU]</b>	42-45	38.5-41.5
<b>Current speed max. [m s<sup>-1</sup>]</b>	0.21	0.3
<b>Current speed average [m s<sup>-1</sup>]</b>	0.09	0.1
<b>Tidal cycle</b>	Semi-diurnal (0.37 dbar, 3 cm s <sup>-1</sup> )	Semi-diurnal (0.6 dbar, 8.2 cm s <sup>-1</sup> )
<b>Average pH</b>	8.01	8.12

951

952 **Table 3** Tidal analysis of the ALBEX lander from 6 m above the sea floor. Depth, mean current speed, mean current direction,  
 953 tidal prediction of pressure fluctuations, two most important harmonics with amplitude, tidal prediction of horizontal current  
 954 field, two most important harmonics with semi-major axis' amplitude.

	Station no. (GeoB ID)	Depth (m)	Mean current speed (cm s <sup>-1</sup> )	Current direction (°)	Tides [%] (p)	Const. [dbar]	Tides [%] (u)	Const. [cm s <sup>-1</sup> ]
<b>Namibia</b>	20507-1	430	9.34	221.6	81.8	M2: 0.37	10.5	M2: 3.1 M3: 0.8
<b>Angola</b>	20921-1	340	9.96	247.9	91.6	M2: 0.59 M3: 0.04	36	M2: 7.8 M8: 0.7
	20940-1	530	8.92	275.6	86.8	M2: 0.60 M8: 0.02	50.9	M2: 8.6 M3: 3.7

955

